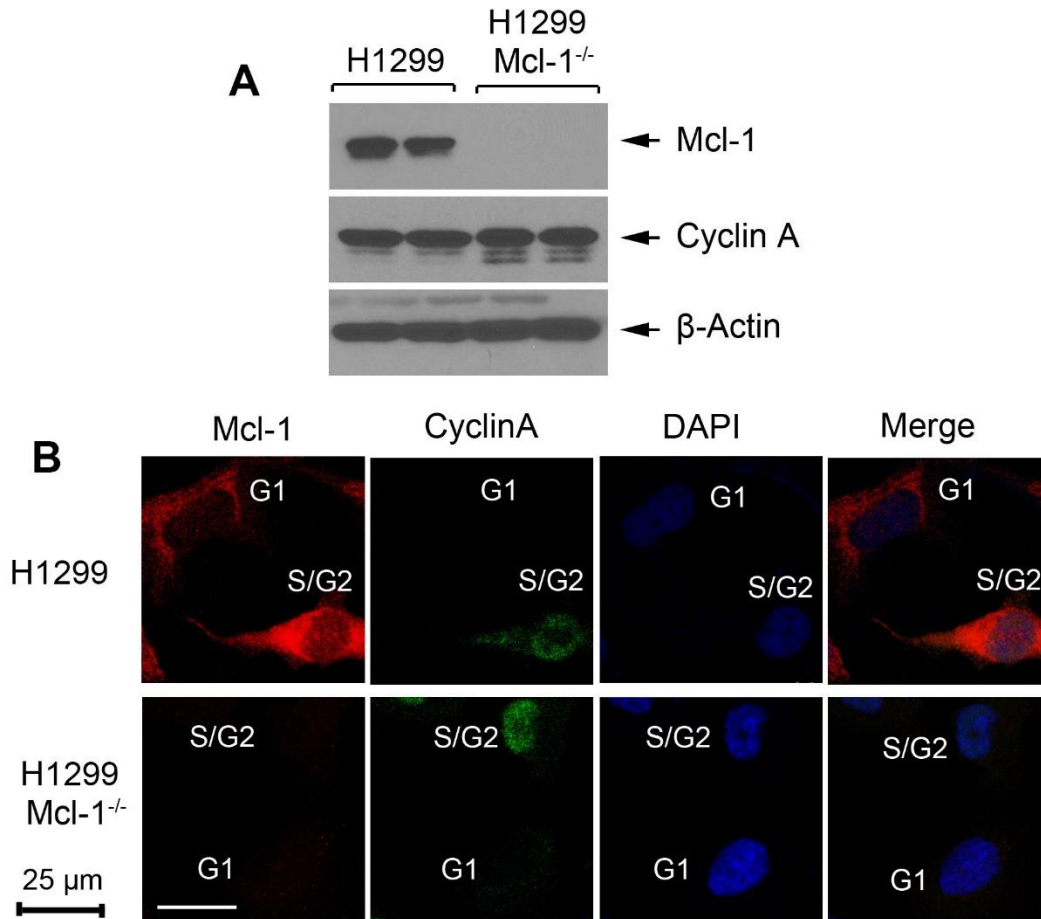
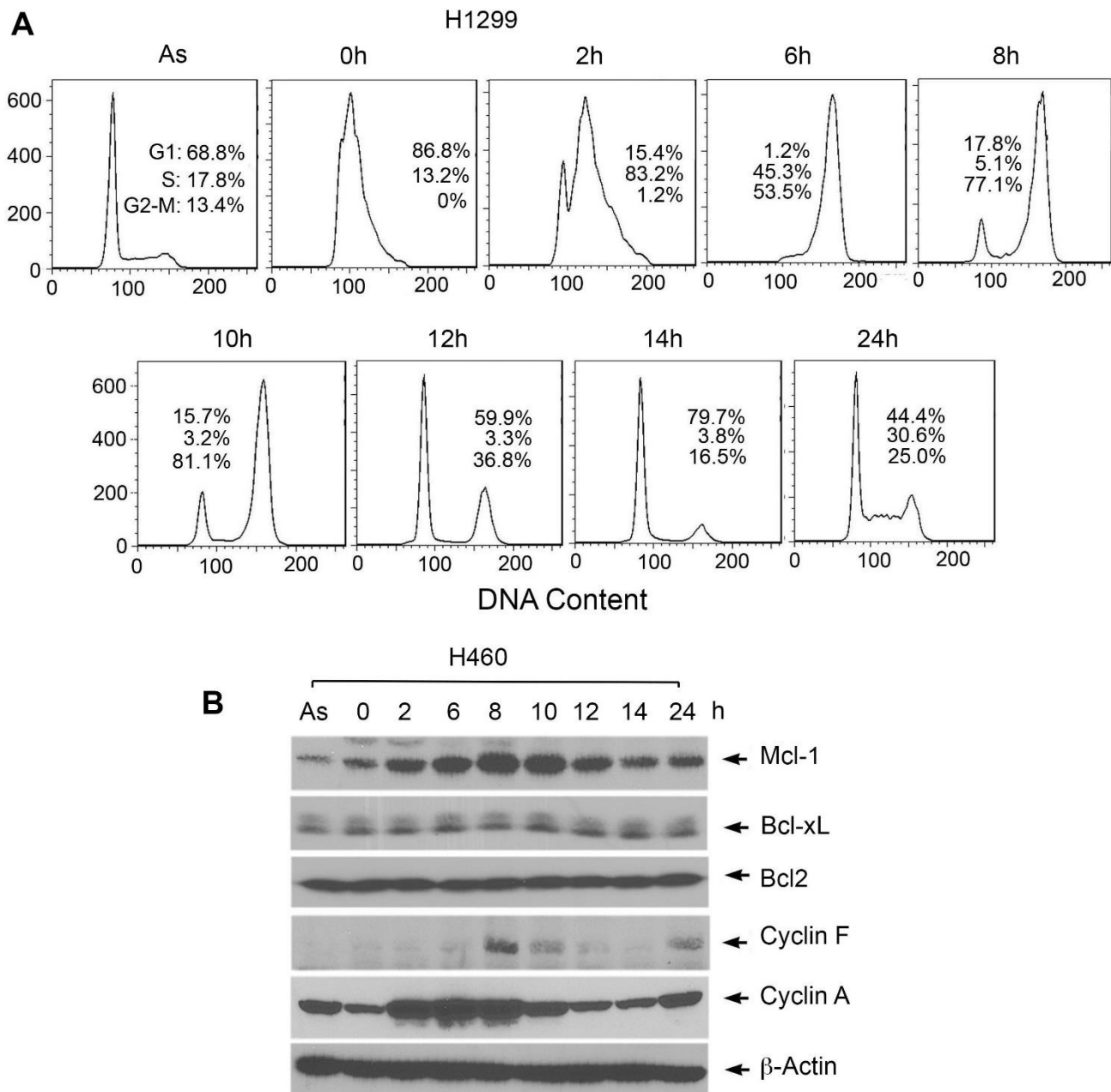


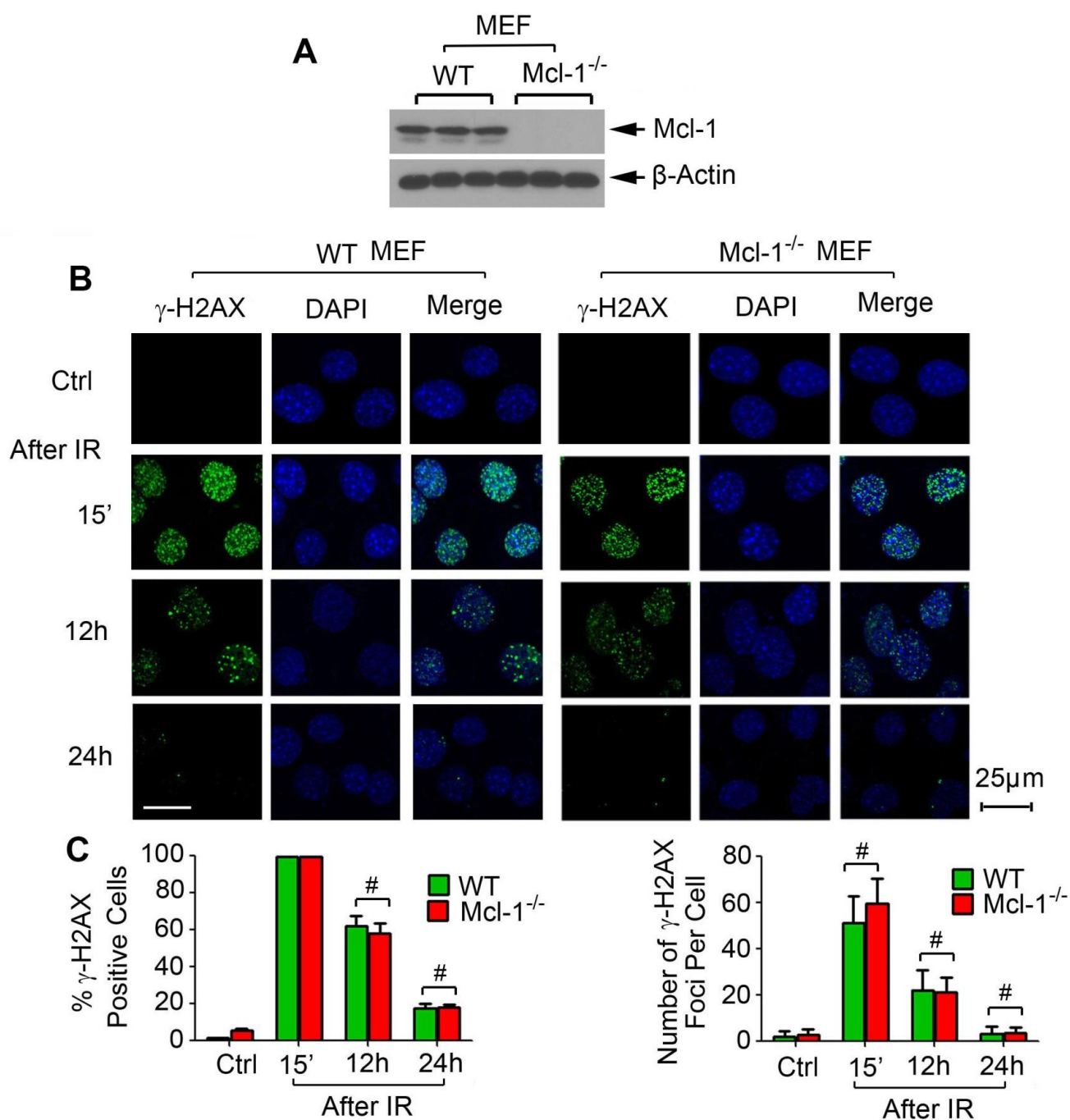
Supplemental Data and Supplemental Methods



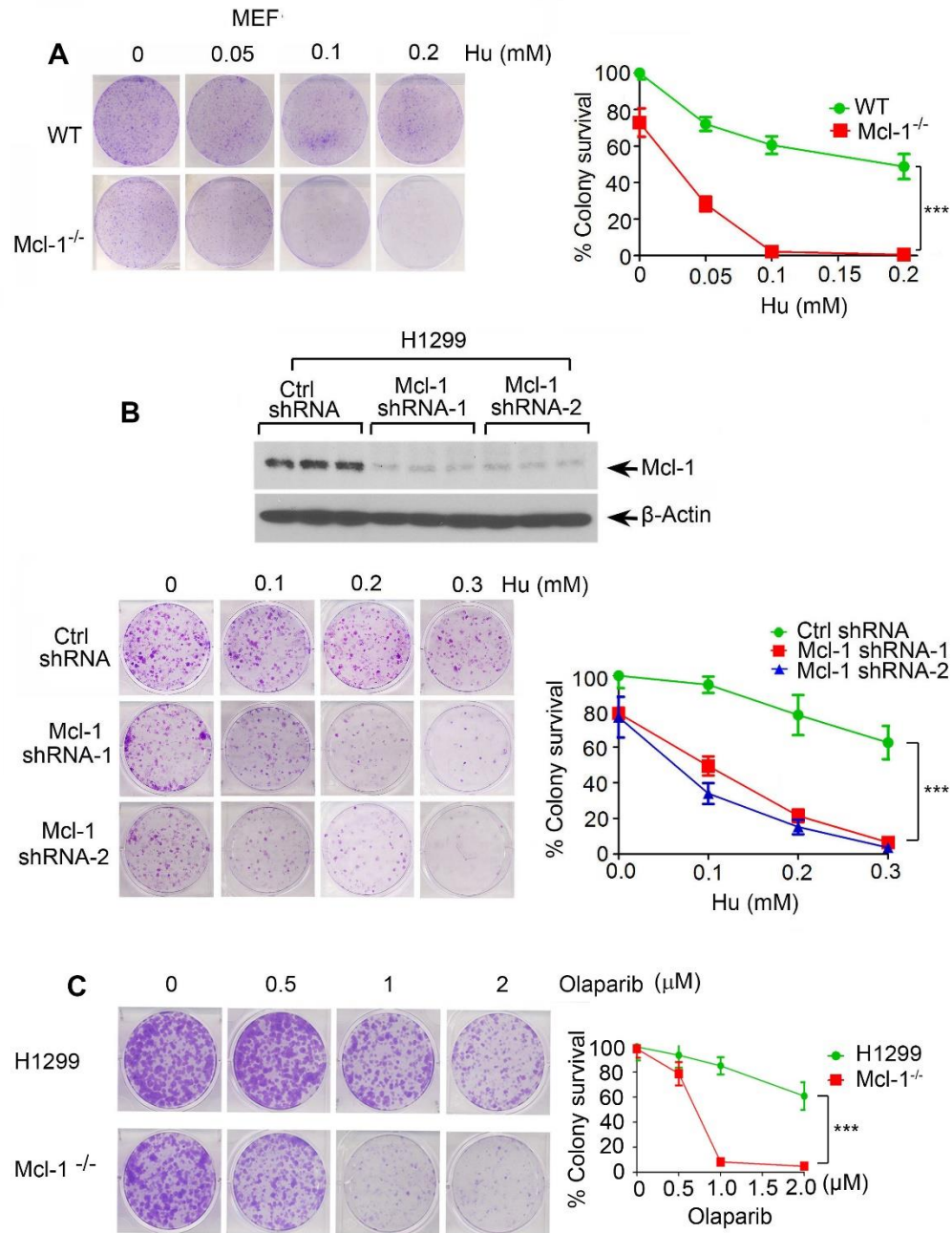
Supplemental Figure 1. Mcl-1 was specifically knocked out from H1299 cells using the CRISPR/Cas9 system. (A) Expression of Mcl-1 or Cyclin A in H1299 or H1299 Mcl-1^{-/-} cells was detected by Western blot using a Mcl-1 or Cyclin A antibody, respectively. (B) Mcl-1 and Cyclin A levels in H1299 or H1299 Mcl-1^{-/-} cells were measured by immunofluorescence using Mcl-1 and Cyclin A antibodies. The scale bar represents 25μm. Since both Western blot and immunofluorescence only detected Mcl-1 in H1299 but not in H1299 Mcl-1^{-/-} cells, these results confirmed that the Mcl-1 antibody used in these experiments is specific for the detection of Mcl-1.



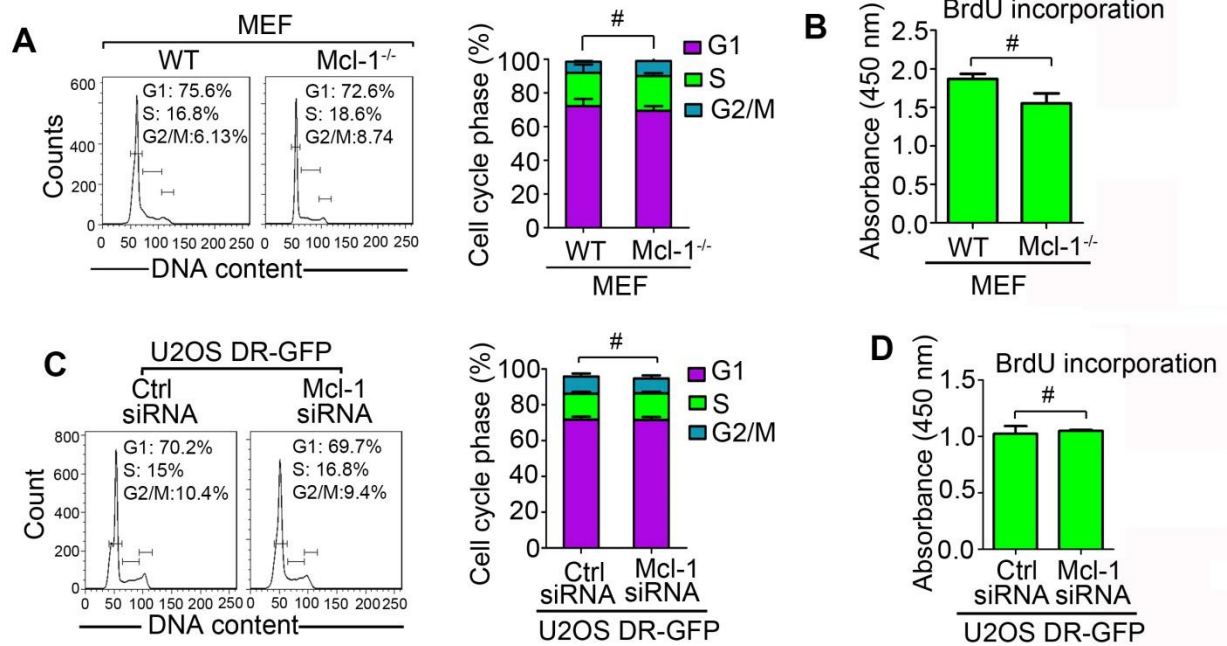
Supplemental Figure 2. (A) H1299 cells were synchronized by double-thymidine block. After washing off thymidine, cells were released to normal medium for a time course up to 24h. Cell cycle was analyzed by FACS. “As” is used as the abbreviation for asynchronous cells. **(B)** Expression panel of Mcl-1 during cell cycle progression in H460 cells. H460 cells were synchronized by double-thymidine block. After washing off thymidine, cells were released to normal culture medium for a time course up to 24h. Mcl-1, Bcl2, Bcl-xL, cyclin A and cyclin F were analyzed by Western blot. “As” is used as the abbreviation for asynchronous cells.



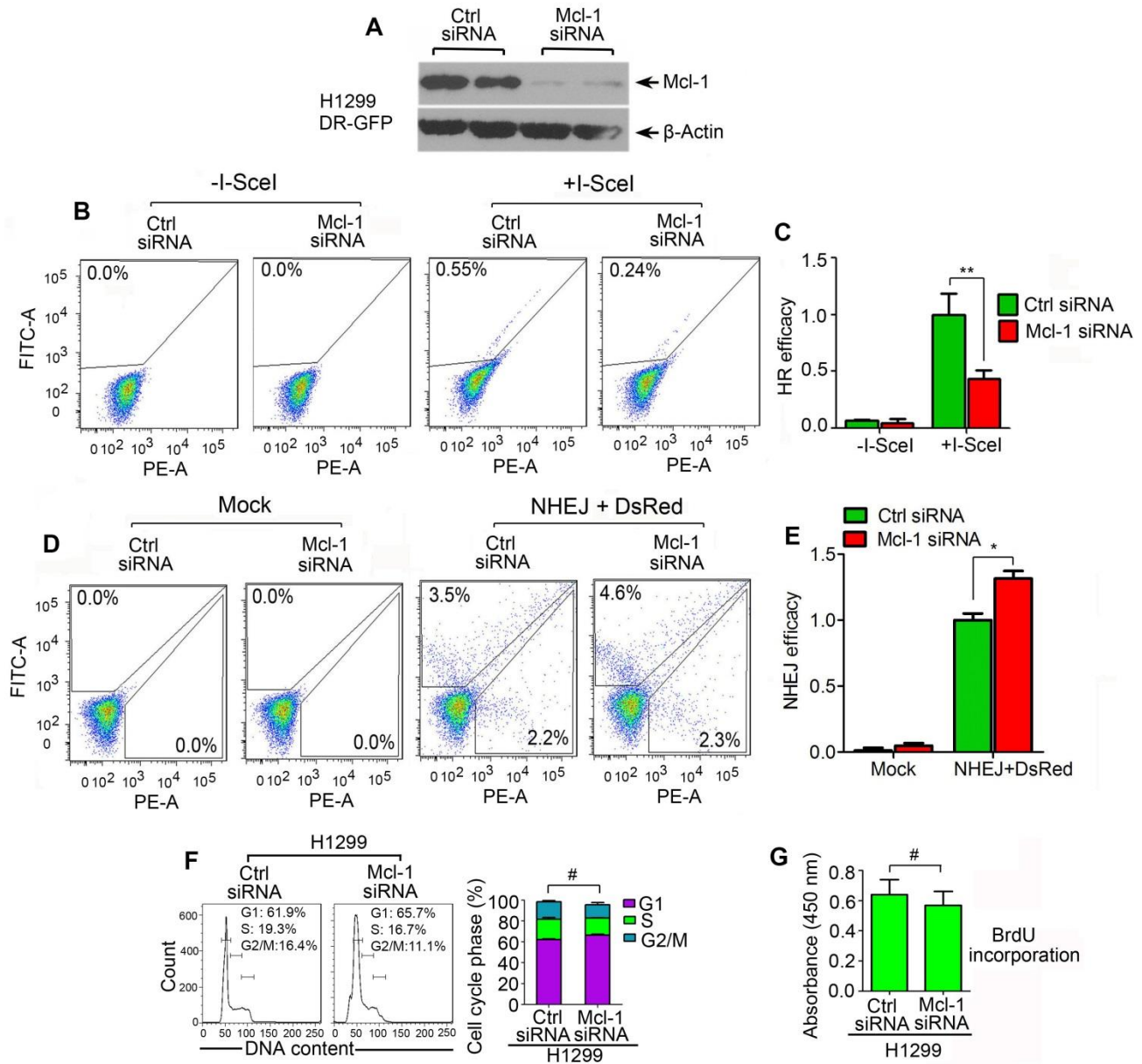
Supplemental Figure 3. Effects of Mcl-1 loss on the repair of IR-induced DSBs. (A) Western blot for analysis of Mcl-1 protein expression in Wild type (WT) and Mcl-1^{-/-} MEFs. **(B)** WT and Mcl-1^{-/-} MEFs were exposed to 1Gy of IR and harvested at various time points. DSBs were analyzed by immunostaining using γ -H2AX. The scale bar represents 25 μ m. **(C)** The percentage of γ -H2AX positive cells (≥ 5 foci) (left panel) and the number of γ -H2AX foci per cell (right panel) were determined by counting at least 100 cells from each sample. Data represent the mean \pm SD, n=3 per group. #*P* > 0.05, by 2-tailed *t*-test.



Supplemental Figure 4. Effects of Mcl-1 loss on clonogenic survival following treatment with DNA replication stress agents (hydroxyurea or olaparib). (A) WT and Mcl-1^{-/-} MEF cells were treated with increasing concentrations of hydroxyurea (Hu), followed by colony formation assay. Data represent the mean \pm SD, $n=3$ per group. *** $P < 0.001$, by 2-tailed t -test. (B) Mcl-1 was knocked down in H1299 cells using Mcl-1 shRNA1, Mcl-1 shRNA2 or Ctrl shRNA. Cells were then treated with increasing concentrations of Hu, followed by colony formation assay. Data represent the mean \pm SD, $n=3$ per group. *** $P < 0.001$, by 2-tailed t -test. (C) H1299 parental and H1299 Mcl-1^{-/-} cells were treated with increasing concentrations of olaparib, followed by colony formation assay. Data represent the mean \pm SD, $n=3$ per group. *** $P < 0.001$, by 2-tailed t -test.



Supplemental Figure 5. Effects of Mcl-1 loss on cell cycle and cell proliferation. (A) and (B) Cell cycle and cell proliferation rate were analyzed in WT and Mcl-1^{-/-} MEFs. Data represent the mean \pm SD, n=3 per group. # $P > 0.05$, by 2-tailed *t*-test. (C) and (D) Mcl-1 was knocked down using Mcl-1 siRNA from DR-GFP-U2OS cells, followed by analysis of cell cycle and cell proliferation rate. Data represent the mean \pm SD, n=3 per group. # $P > 0.05$, by 2-tailed *t*-test.



Supplemental Figure 6. Silencing of Mcl-1 using Mcl-1 siRNA results in decreased HR and increased NHEJ in H1299 cells. (A) Mcl-1 expression was analyzed by Western blot in H1299 cells expressing Ctrl siRNA and Mcl-1 siRNA. (B) and (C) HR activity was compared in H1299 cells expressing Mcl-1 siRNA or Ctrl siRNA. Data represent the mean \pm SD, $n=3$ per group. $**P < 0.01$, by 2-tailed t -test. (D) and (E) NHEJ activity was compared in H1299 cells expressing Mcl-1 siRNA or Ctrl siRNA. Data represent the mean \pm SD, $n=3$ per group. $*P < 0.05$, by 2-tailed t -test. (F) and (G) Cell cycle and cell proliferation rate were compared in H1299 cells expressing Mcl-1 siRNA or Ctrl siRNA. Data represent the mean \pm SD, $n=3$ per group. $\#P > 0.05$, by 2-tailed t -test.

Supplemental Table 1. Plating efficiency (PE) of H1299 and Mcl-1^{-/-} H1299 cells

No. of cells plated	1×10 ³		2×10 ³		4×10 ³		6×10 ³	
	H1299	Mcl-1 ^{-/-}	H1299	Mcl-1 ^{-/-}	H1299	Mcl-1 ^{-/-}	H1299	Mcl-1 ^{-/-}
No. of colonies	172±12	166±21	372±29	358±20	942±49	887±84	1288±87	1231±68
PE	17.2±1.2	16.6±2.1 ^e	18.6±1.4	17.9±1 ^f	23.5±1.2	22.1±2 ^g	21.4±1.4	20±1 ^h

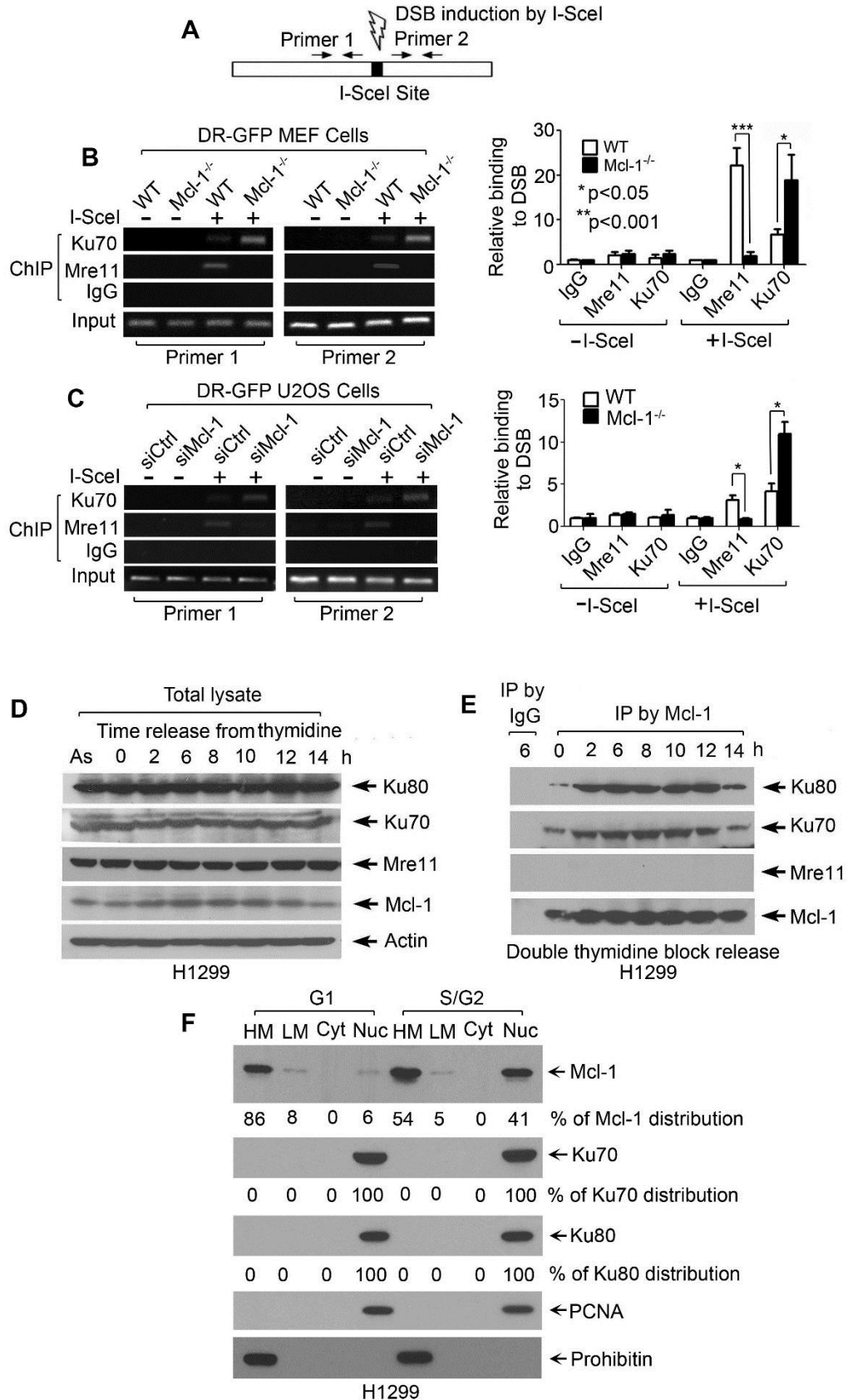
^ap=0.37 (H1299 vs. Mcl-1^{-/-}); ^bp=0.27 (H1299 vs. Mcl-1^{-/-}); ^cp=0.26 (H1299 vs. Mcl-1^{-/-}); ^dp=0.19 (H1299 vs. Mcl-1^{-/-})

Supplemental Table 2. Plating efficiency (PE) of WT or Mcl-1^{-/-} MEF cells

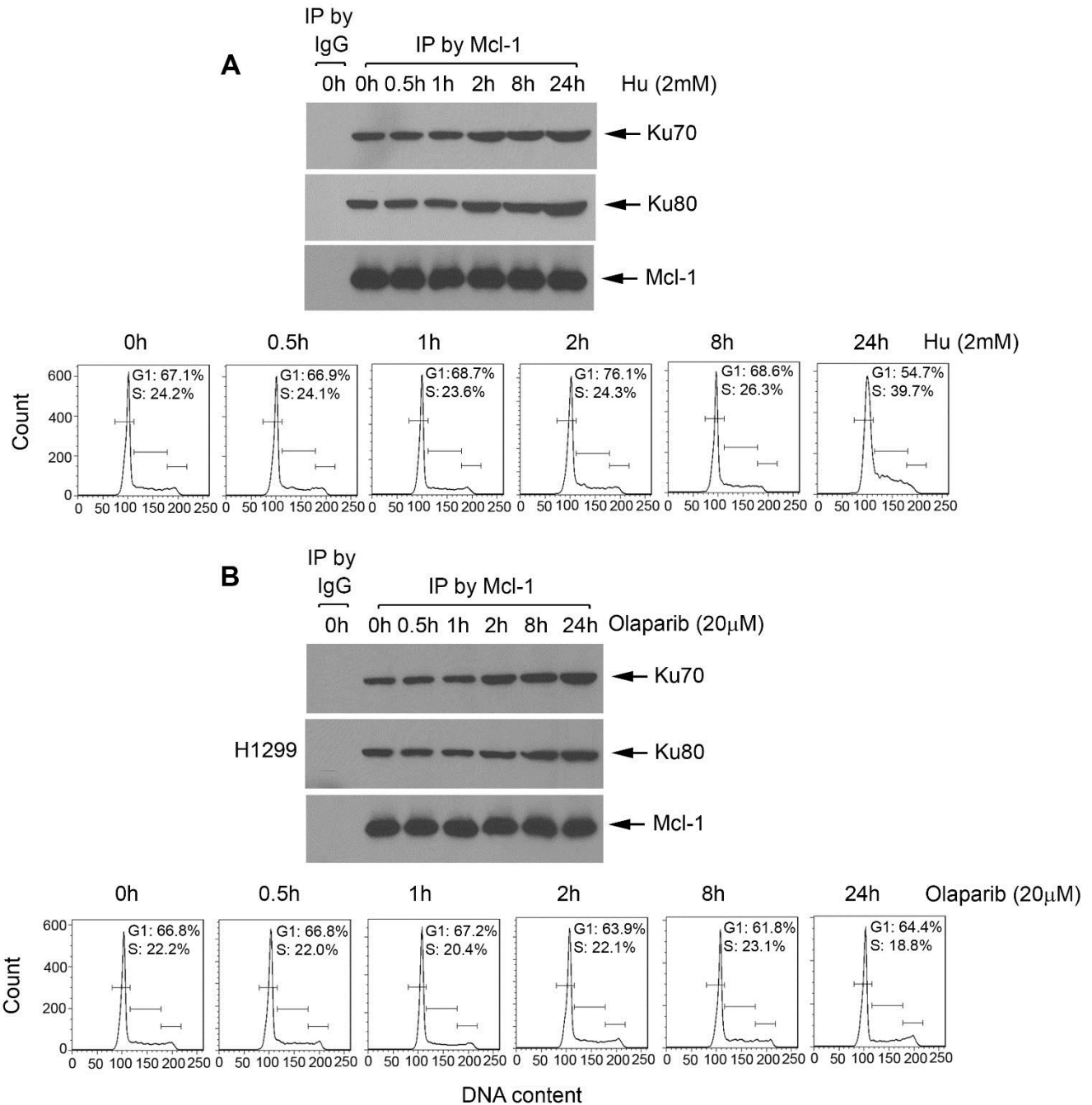
No. of cells plated	1×10 ³		2×10 ³		4×10 ³		6×10 ³	
	WT	Mcl-1 ^{-/-}						
No. of colonies	485±90	428±43	854±44	789±77	1233±45	1107±160	1847±156	1676±107
PE	48.5±9.0	42.8±4.3 ^a	42.7±2.2	39.4±3.8 ^b	30.8±1.1	27.7±4.0 ^c	30.7±2.6	27.9±1.8 ^d

^ep=0.67 (WT vs. Mcl-1^{-/-}); ^fp=0.53 (WT vs. Mcl-1^{-/-}); ^gp=0.39 (WT vs. Mcl-1^{-/-}); ^hp=0.42 (WT vs. Mcl-1^{-/-})

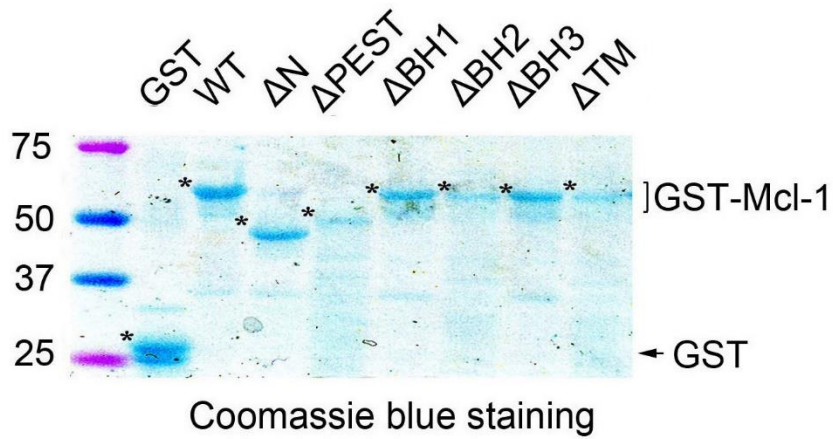
Plating efficiency experiments were carried out using four dilutions of cells (1×10³, 2×10³, 4×10³, and 6×10³), each in triplicate, as indicated above. Knockout of Mcl-1 from H1299 or MEF cells did not significantly affect plating efficiency compared to control cells. Data represent the mean ± SD, n=3 per group. *P* values were determined by 2-tailed *t*-test.



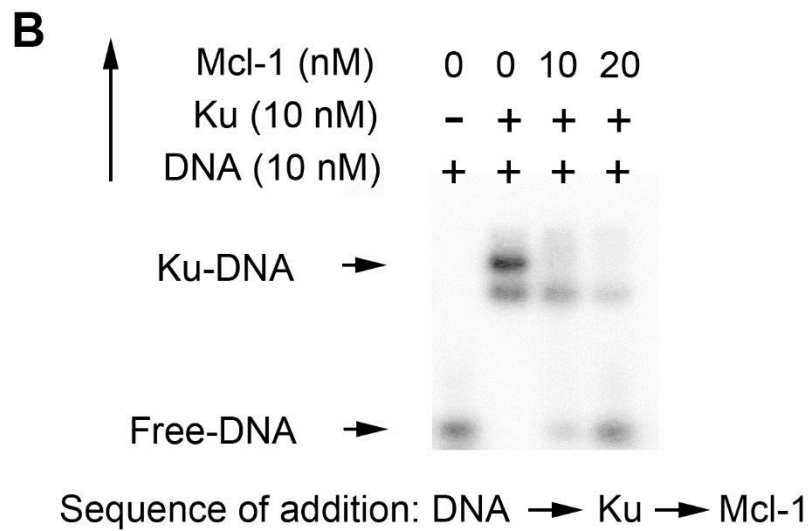
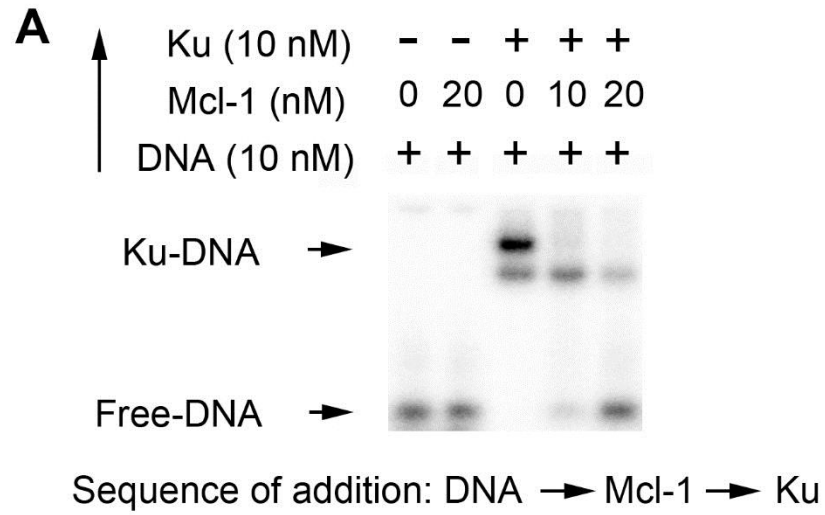
Supplemental Figure 7. Mcl-1 is essential for recruitment of Mre11 to DSBs via direct interaction with Ku. (A) Schematic representation of the position of primers used for conventional PCR examination for ChIP, primer 1 locates 200 bp upstream from the I-SceI site, primer 2 locates 200 bp downstream from the I-SceI site. (B) The pDR-GFP plasmid was stably transfected into WT and Mcl-1^{-/-} knockout MEFs, followed by screening of single copy. Cells were transfected using pCBASceI constructs. ChIP assay was carried out using Ku70 or Mre11, followed by PCR analysis using primer 1 and primer 2 to measure DNA fragments containing DSBs. Data represent the mean \pm SD, n=3 per group. * P < 0.05 and *** P < 0.001, by 2-tailed t -test. (C) Mcl-1 was depleted from DR-GFP U2OS cells using Mcl-1 siRNA, followed by similar ChIP assay. Data represent the mean \pm SD, n=3 per group. * P < 0.05, by 2-tailed t -test. (D) Western blot analysis of Ku proteins, Mre11 and Mcl-1 during cell cycle progression following double thymidine block synchronization. As: asynchronous cells. (E) H1299 cells were synchronized by double-thymidine block. After washing, cells were released to normal medium for a time course up to 24h. Co-IP experiments were performed to measure Mcl-1/Ku or Mcl-1/Mre11 binding. (F) G1 and S/G2 phase H1299 cells were isolated from double thymidine block synchronization. Subcellular fractionation experiments were then performed to isolate heavy membrane (HM) containing mitochondria, light membrane (LH) containing endoplasmic reticulum (ER) and nuclear (Nuc) fractions from G1 or S/G2 phase H1299 cells, respectively. Levels of Ku70 and Mcl-1 in each fraction were analyzed by Western blot and quantified by ImageJ software. To verify the purity of the subcellular fractions obtained, fraction-specific proteins were assessed by probing the same filters. Prohibitin, an exclusively mitochondrial protein (1), was detected only in the mitochondrial fraction, while proliferating cell nuclear antigen (PCNA), a nuclear marker (2), was detected exclusively in the nuclear fraction (Nuc), indicating that the fractionation procedure does not cause cross-contamination between the fractions.



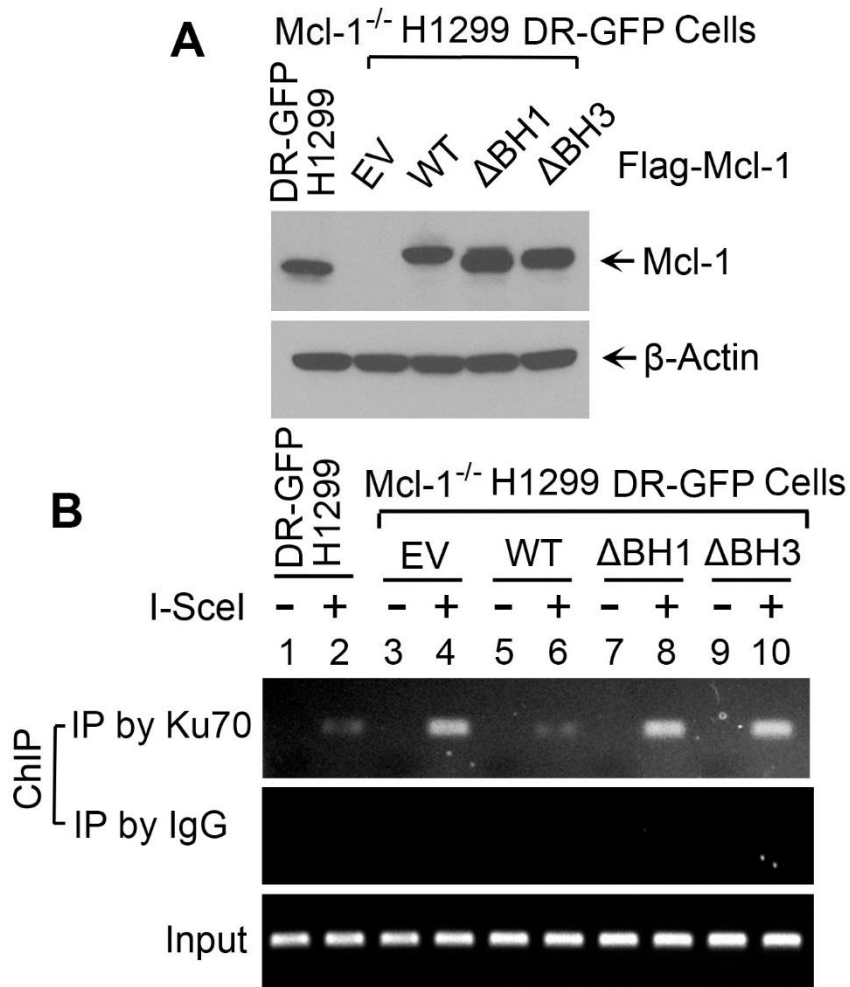
Supplemental Figure 8. Effect of DNA replication stress on interaction between Mcl-1 and Ku proteins. H1299 cells were treated with 2mM of Hydroxyurea (Hu) (**A**) or 20 μ M of olaparib (**B**) for various times (0, 0.5h, 1h, 2h, 8h or 24h). Co-IP experiments for measurement of Mcl-1/Ku interactions were carried out using Mcl-1 antibody. Cell cycle was also analyzed simultaneously at each time point.



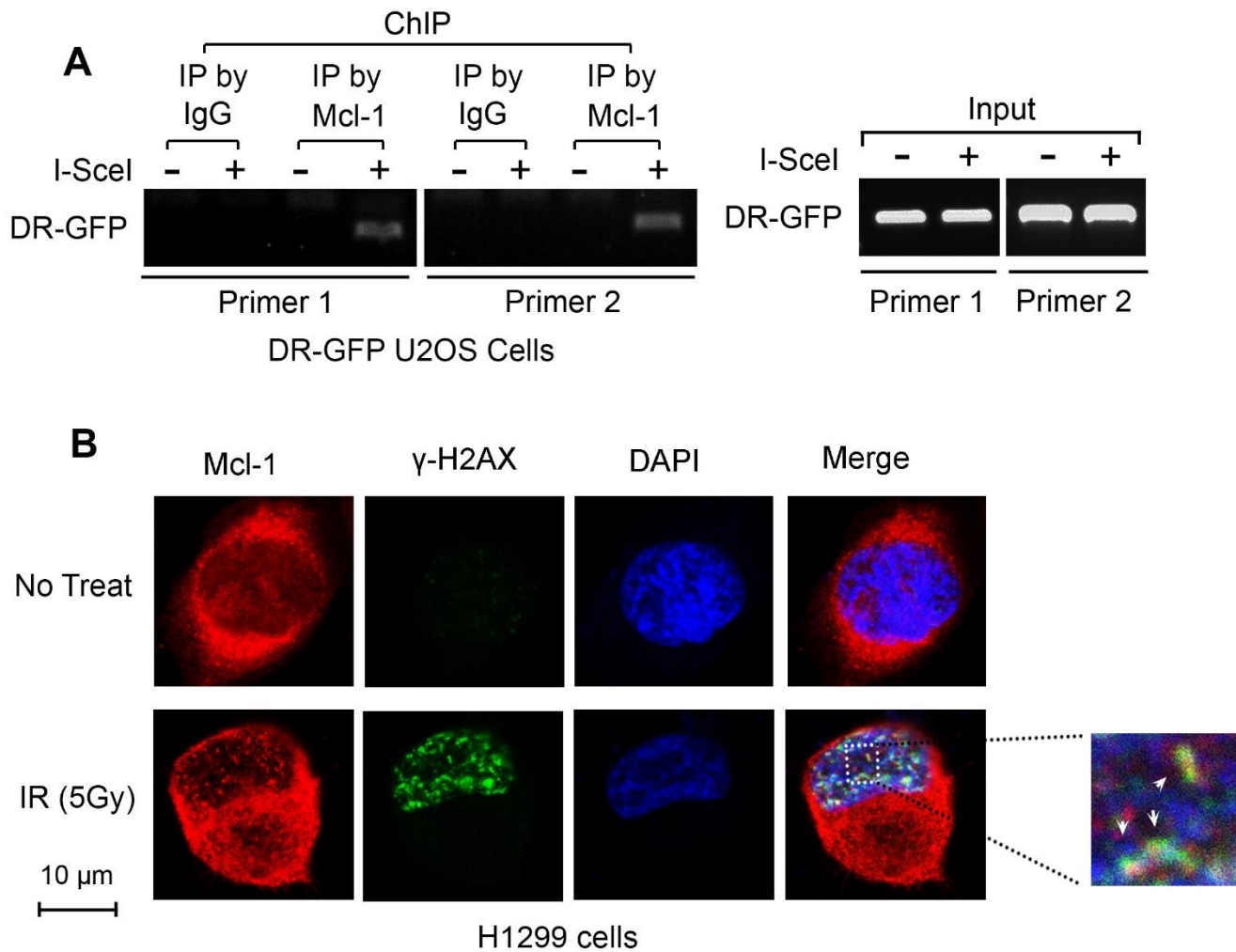
Supplemental Figure 9. Generation and purification of recombinant WT or various Mcl-1 deletion mutant proteins. Coomassie blue staining analysis of recombinant GST-Mcl-1 WT or a series of Mcl-1 deletion mutant proteins generated from *Escherichia coli* Rosetta and purified using a glutathione sepharose column.



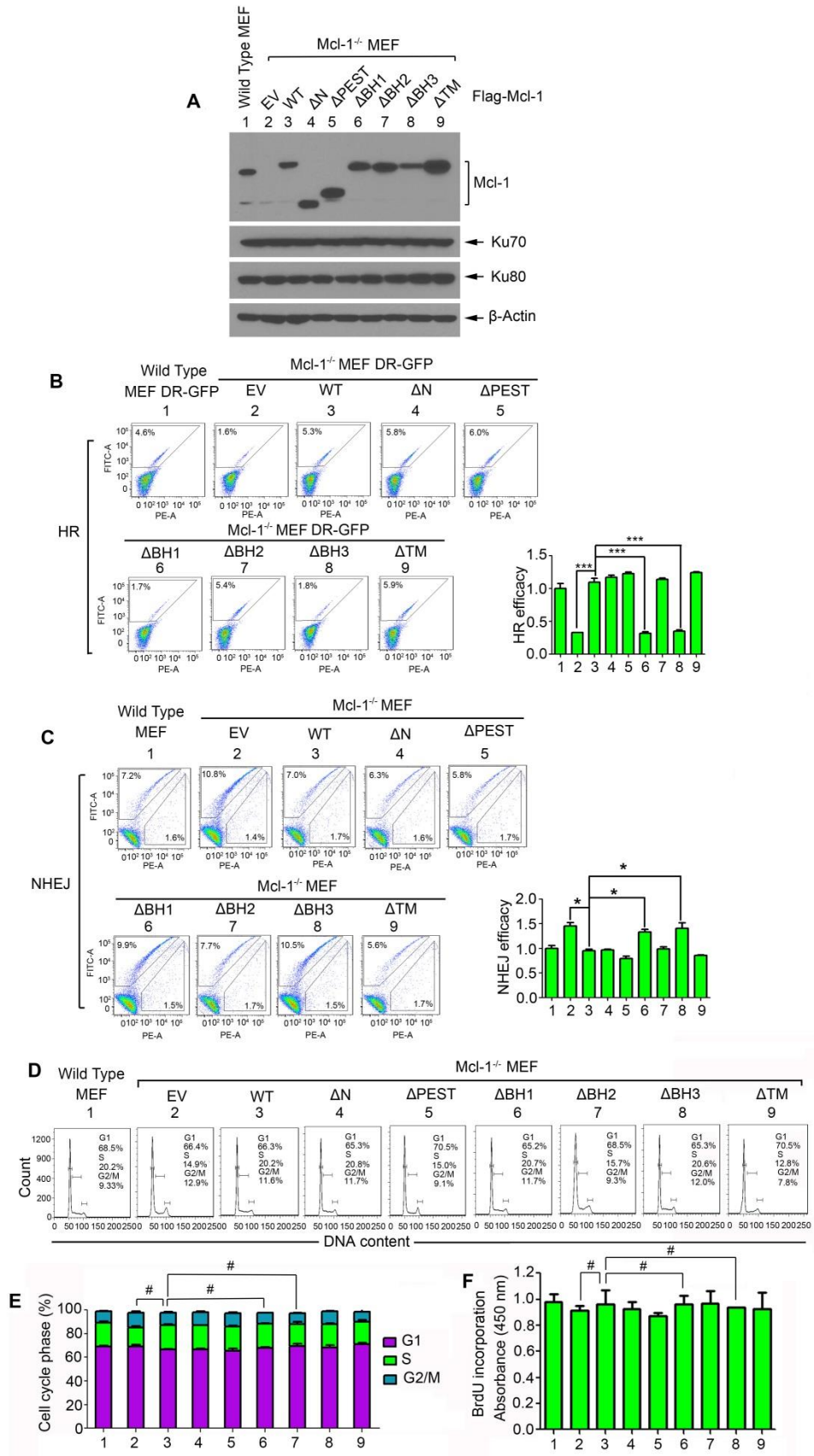
Supplemental Figure 10. Effect of Mcl-1 protein on Ku/DNA binding in vitro. The 5'-end labeled overhang DNA was incubated with Mcl-1 and Ku using two different orders of addition (i.e. DNA → Mcl-1 → Ku, or DNA → Ku → Mcl-1). The Ku/DNA complex was analyzed by EMSA. Similar results were obtained.



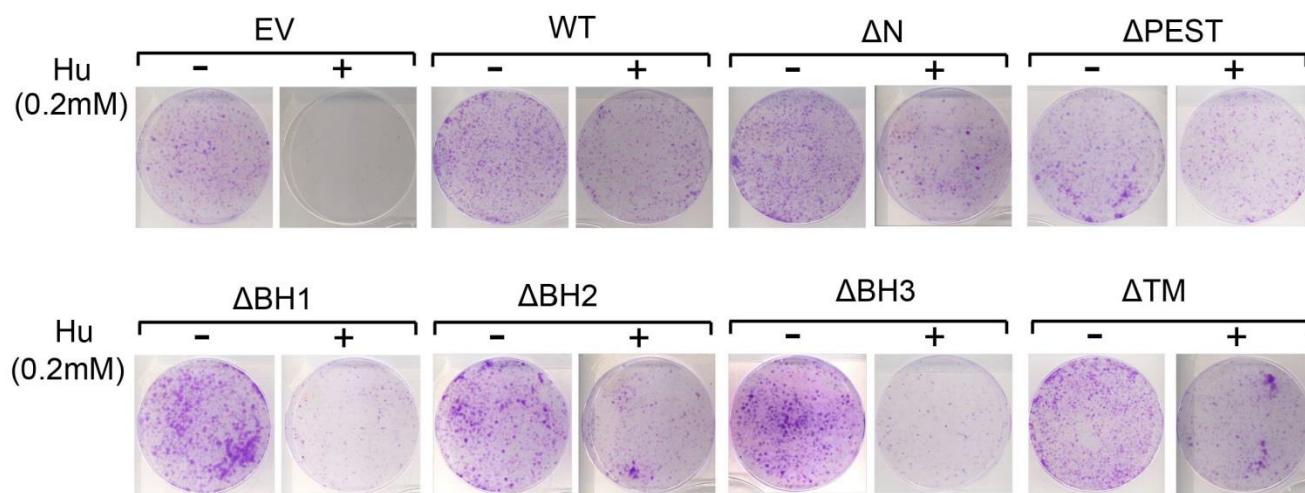
Supplemental Figure 11. Ku binding deficient Mcl-1 mutants failed to prevent Ku recruitment to DSBs. (A) Empty vector, WT Mcl-1, ΔBH1 and ΔBH3 Mcl-1 mutants were transfected into Mcl-1^{-/-} H1299 DR-GFP cells. Mcl-1 expression was analyzed by Western blot. (B) DR-GFP H1299 cells and Mcl-1^{-/-} H1299 DR-GFP cells expressing exogenous WT or ΔBH1, ΔBH3 Mcl-1 deletion mutant were transfected with I-SceI to produce DSBs. ChIP experiments to measure Ku recruitment to DSBs were performed using anti-Ku70 antibody.



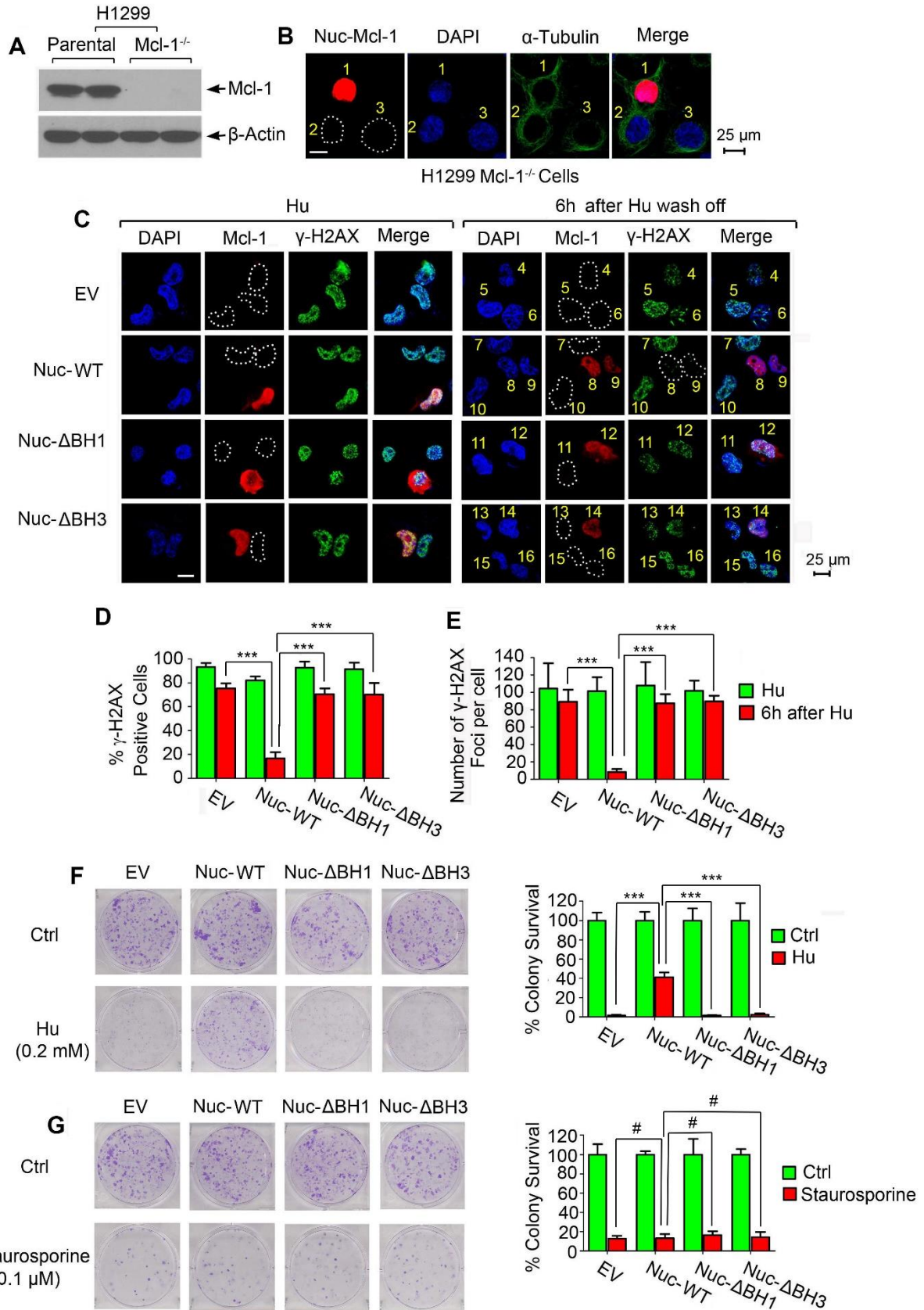
Supplemental Figure 12. Mcl-1 molecules were recruited to DSB sites following DNA double-strand breaks. (A) I-SceI was transfected into DR-GFP U2OS cells to induce DSBs, followed by ChIP using Mcl-1 antibody and PCR using primer 1 and primer 2 as described in “Supplemental Figure 6A” to detect Mcl-1-associated DSBs. (B) S/G2 phase H1299 cells harvested at 6h after double thymidine block were exposed to IR (5Gy), followed by co-staining with Mcl-1 and γ -H2AX. The scale bar represents 10 μ m. Data show that Mcl-1 molecules were mainly enriched on DSB sites to form foci and were co-localized with γ -H2AX (*i.e.* a classic DSB marker).



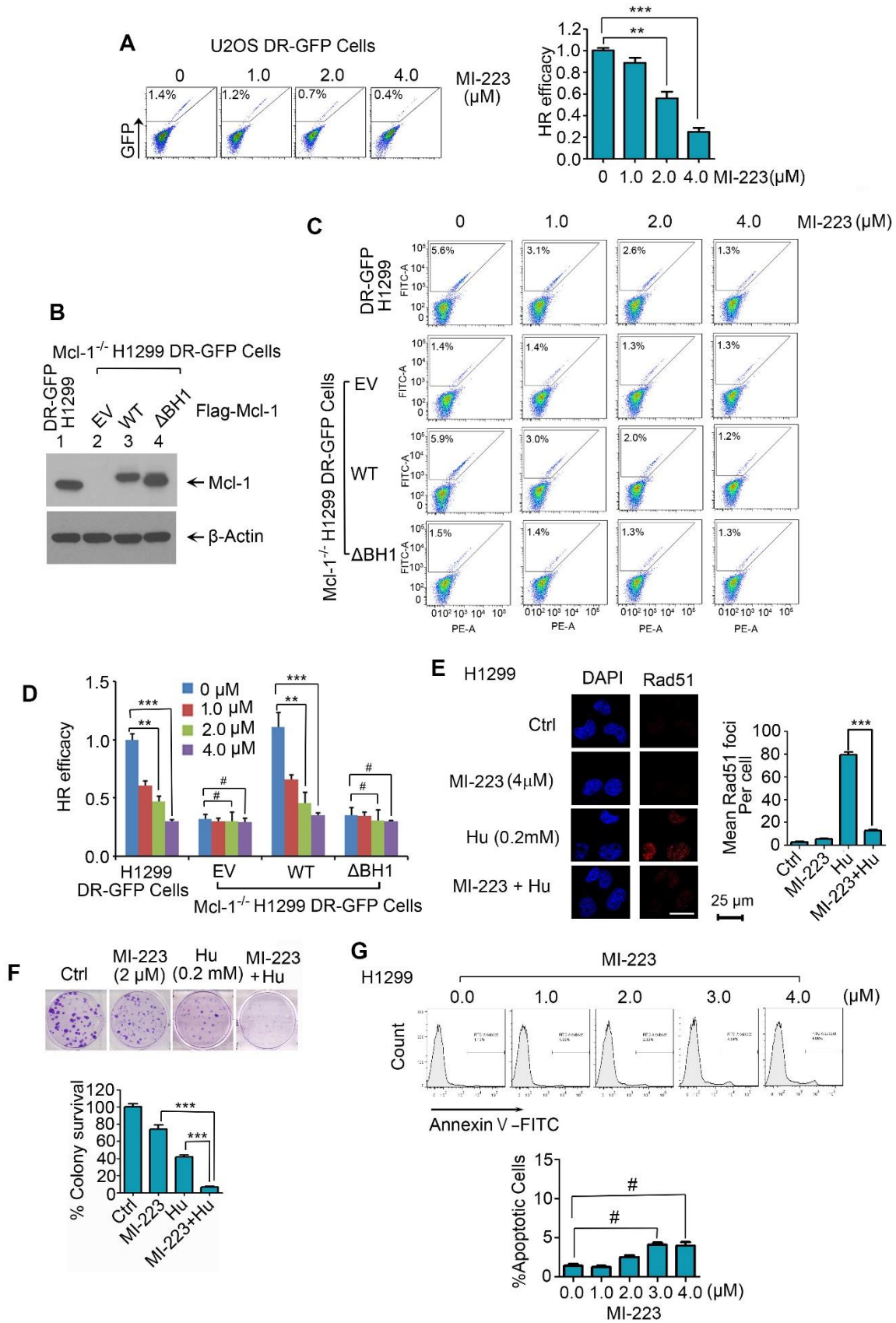
Supplemental Figure 13. Effect of WT or various Mcl-1 deletion mutants on HR and NHEJ. (A) Expression levels of the endogenous Mcl-1 in intact wild type MEF cells and exogenously expressed WT or Mcl-1 deletion mutants or empty vector (EV) control in Mcl-1^{-/-} MEF cells were simultaneously analyzed by Western blot using a Mcl-1 antibody. (B) HR activity was measured and quantified in wild type MEF cells expressing endogenous Mcl-1 and Mcl-1^{-/-} MEF cells expressing exogenous WT or various Mcl-1 deletion mutants. Data represent the mean \pm SD, n=3 per group. *** $P < 0.001$, by 2-tailed t -test. (C) After transfection of cells with NHEJ reporter, NHEJ activity was measured and quantified in wild type MEF cells expressing endogenous Mcl-1 and Mcl-1^{-/-} MEF cells expressing exogenous WT or various Mcl-1 deletion mutants. Data represent the mean \pm SD, n=3 per group. * $P < 0.05$, by 2-tailed t -test. (D), (E) and (F) Cell cycle and proliferation rate were analyzed in wild type MEF cells expressing endogenous Mcl-1 and Mcl-1^{-/-} MEF cells expressing exogenous WT or various Mcl-1 deletion mutants. Data represent the mean \pm SD, n=3 per group. # $P > 0.05$, by 2-tailed t -test.



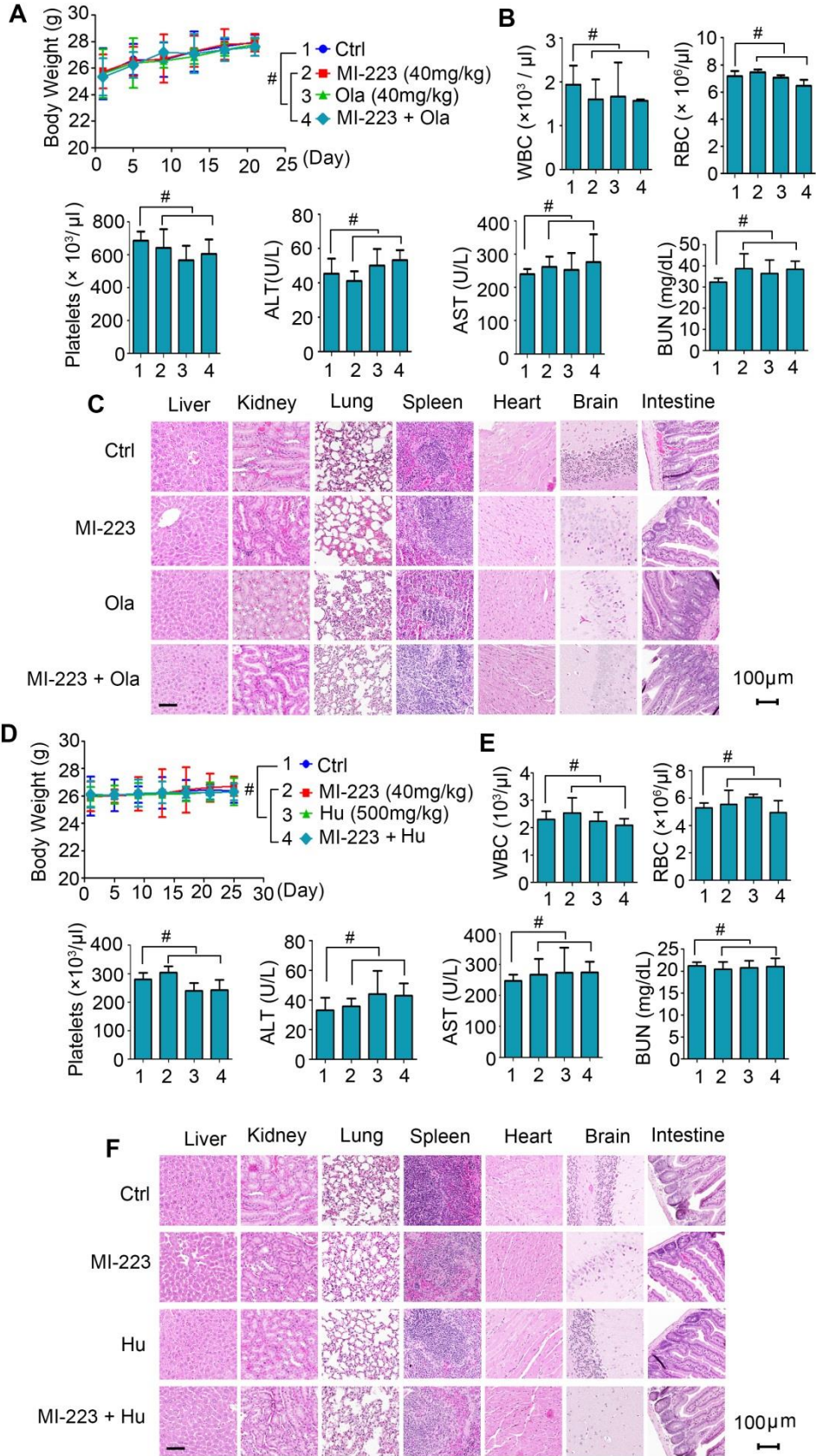
Supplemental Figure 14. Effect of exogenous expression of WT or individual Mcl-1 deletion mutants on clonogenic cell survival following Hu treatment. MEF Mcl-1^{-/-} cells expressing exogenous WT or individual Mcl-1 deletion mutant(s) were treated with 0.2mM Hu, followed by colony formation analysis.



Supplemental Figure 15. Nuclear-targeted Mcl-1 promotes HR-dependent DSB repair and prolongs clonogenic survival following exposure of cells to Hu but not staurosporine. (A) Mcl-1 was knocked out from H1299 cells using CRISPR/Cas9 system. Mcl-1 expression was confirmed by Western blot. (B) Nuclear-targeted Mcl-1 (Nuc-Mcl-1) constructs were transfected into H1299 Mcl-1 knockout (Mcl-1^{-/-}) cells, followed by co-immunostaining using Mcl-1 and α -tubulin antibodies. The scale bar represents 25 μ m. (C) H1299 Mcl-1^{-/-} cells expressing exogenous Nuc-WT, Nuc- Δ BH1, Nuc- Δ BH3 Mcl-1 mutant were treated with 0.2 mM Hu for 24h. After washing, cells were released into normal medium for another 6h. DSBs were analyzed by immunostaining with γ -H2AX. The Scale bar represents 25 μ m. (D) and (E) The percentage of γ -H2AX positive cells and the number of γ -H2AX foci per cell were determined as above. Data represent the mean \pm SD, n=3 per group. *** P < 0.001, by 2-tailed t -test. (F) Cells were treated with Hu (0.2 mM) for 24h. After washing, cells were cultured in normal medium, followed by colony formation analysis. Data represent the mean \pm SD, n=3 per group. *** P < 0.001, by 2-tailed t -test. (G) Cells were treated with staurosporine (0.1 μ M) for 24h. After washing, cells were cultured in normal medium, followed by colony formation analysis. Data represent the mean \pm SD, n=3 per group. # P > 0.05, by 2-tailed t -test.



Supplemental Figure 16. (A) HR efficiency was analyzed in U2OS DR-GFP cells in the absence or presence of increasing concentrations of MI-223. Data represent the mean \pm SD, n=3 per group. $**P < 0.01$ and $***P < 0.001$, by 2-tailed *t*-test. (B) Expression levels of endogenous Mcl-1 in H1299 DR-GFP cells and exogenously expressed WT or Δ BH1 Mcl-1 deletion mutant or empty vector (EV) control in Mcl-1^{-/-} H1299 DR-GFP cells were simultaneously analyzed by Western blot using Mcl-1 antibody. (C) and (D) H1299 DR-GFP cells expressing endogenous Mcl-1 or Mcl-1^{-/-} H1299 DR-GFP cells expressing exogenous WT or Δ BH1 Mcl-1 deletion mutant or empty vector (EV) control were treated with increasing concentrations of MI-223 for 24h, followed by analysis of HR efficacy. Data represent the mean \pm SD, n=3 per group. $**P < 0.01$, $***P < 0.001$ and $^{\#}P > 0.05$, by 2-tailed *t*-test. (E) H1299 cells were treated with Hu (0.2mM), MI-223 (4 μ M) or in combination for 24h, followed by immunostaining with Rad51 antibody. Rad51 foci were quantified by counting at least 100 cells from each sample. The scale bar represents 25 μ m. Data represent the mean \pm SD, n=3 per group. $***P < 0.001$, by 2-tailed *t*-test. (F) H1299 cells were treated with Hu (0.2 mM), MI-223 (2 μ M) or in combination, followed by colony formation assay. Data represent the mean \pm SD, n=3 per group. $***P < 0.001$, by 2-tailed *t*-test. (G) H1299 cells were treated with increasing concentrations of MI-223 for 48h, followed by Annexin V staining and FACS analysis. Data represent the mean \pm SD, n=3 per group. $^{\#}P > 0.05$, by 2-tailed *t*-test.



Supplemental Figure 17. In vivo toxicity analysis. (A), (B) and (C) After treatment with MI-223, Ola or combination as indicated, body weight, blood test and H&E histology of various organs were analyzed. Data represent the mean \pm SD, n=6 per group. $^{\#}P > 0.05$, by 2-tailed *t*-test. (D), (E) and (F) After treatment with MI-223, Hu or combination as indicated, body weight, blood test and H&E histology of various organs were analyzed. The scale bars represents 100 μ m. Data represent the mean \pm SD, n=6 per group. $^{\#}P > 0.05$, by 2-tailed *t*-test.

Supplemental Methods

Materials.

Anti-human Mcl-1 (catalog sc-819), Ku70 (catalog sc-55505), Ku80 (catalog sc-5280), β -actin (catalog sc-47778), cyclin F (catalog sc-952), HA (catalog sc-7392), GST (catalog sc-138), PCNA (catalog sc-25280), cyclin A for immunofluorescence (catalog sc-271682) and prohibitin (catalog sc-377037) antibodies were purchased from Santa Cruz Biotechnology (Santa Cruz, CA). Anti-mouse Mcl-1 antibody (catalog 600-401-394) was obtained from Rockland Immunochemicals (Gilbertsville, PA). Anti- γ -H2AX (catalog 05-636, clone JBW301), Rad51 (catalog PC130) and RPA32 (catalog NA18, clone Ab-2) antibodies were purchased from EMD Millipore (Billerica, MA). Anti-Bcl2 (catalog 2870, clone 50E3) and Mre11 (catalog 4895) were purchased from Cell Signaling Technology (Danvers, MA). Cyclin A for Western blot (catalog ab38, clone E23.1), Bcl-xL (catalog ab32370) and Ki67 (catalog ab15580) antibodies were obtained from Abcam (Cambridge, UK). Anti-Flag antibody (catalog F3165, clone M2) was purchased from Sigma (St. Louis, MO). Anti-phospho RPA32 S4/8 antibody (catalog A300-245A) was obtained from Bethyl Laboratories (Montgomery, TX). Alexa Fluor 488 goat anti-mouse (catalog A10680) and Alexa Fluor 555 goat anti-rabbit (catalog A21429) were purchased from Life Technologies (Carlsbad, CA). Small molecule NSC320223 (MI-223) was obtained from the Drug Synthesis and Chemistry Branch, Developmental Therapeutic Program, Division of Cancer Treatment and Diagnosis, National Cancer Institute (NCI, Bethesda, MD) (<http://dtp.nci.nih.gov/RequestCompounds>). MG132 was purchased from EMD chemicals, Inc. (Darmstadt, Germany). SYBR Green Supermix was obtained from Bio-Rad (Hercules, CA). MEF1 nucleofector kit was purchased from Lonza (Basel, Swiss). Purified Ku70/80 complex was obtained from Trevigen (Gaithersburg, MD). [γ - 32 P] ATP was purchased from PerkinElmer (Waltham, MA). All oligonucleotides were obtained from Integrated DNA Technologies (Coralville, IA). Hydroxyurea and thymidine were purchased from Sigma (St. Louis, MO). Olaparib was obtained from Selleckchem (Houston, TX). All reagents used were obtained from commercial sources unless otherwise stated.

Immunofluorescence.

Cells were grown on chamber slides (BD Falcon, MA), washed with cold 1 \times PBS, fixed with 4.0% paraformaldehyde in 1 \times PBS for 10 min at room temperature, and permeabilized with 0.5% Triton X-100 in 1 \times PBS for 15 min. After blocking with 10% normal goat serum (Life technologies, Carlsbad, CA) for 1h, samples were incubated with the indicated primary antibody at 4 $^{\circ}$ C overnight. After washing, samples were incubated with Alexa Fluor 488 goat anti-mouse IgG (green) or Alexa Fluor 555 goat anti-rabbit IgG (red) for 45 min at room temperature in the dark. After washing, samples were mounted with Prolong Gold antifade

reagent containing DAPI (Invitrogen). Images were captured using LSM 510 confocal microscope (Zeiss, Sweden).

Measurement of DSBs by pulsed-field gel electrophoresis.

Pulsed-field gel electrophoresis (PFGE) was performed as previously described (3, 4). Briefly, cells were harvested by trypsinization, and agarose plugs of 1×10^6 cells were prepared with a CHEF disposable plug mold (BioRad) and incubated in lysis buffer (100mM EDTA, 1% sodium laurylsarcosyne, 0.2% sodium deoxycholate, 1mg/ml proteinase K) at 37°C for 48 h. Samples were then washed 2 times with H₂O for 10 min and 4 times with TE buffer (10 mM Tris-HCl (pH 8.0), 100 mM EDTA) before electrophoresis. All washes were performed at 50°C. The electrophoresis was performed at 14°C for 23 h in 0.9% (w/v) SeaKem Gold agarose (Lonza, Rockland, ME) containing 250mM Tris-borate with EDTA (TBE) using a Bio-Rad CHEF DRIII apparatus with the following parameters: 4 volts/cm; 120° linear angle; 30-s initial switch, 5-s final switch. The gel was stained using ethidium bromide and visualized using UV light. Under the electrophoresis conditions used, high molecular weight genomic DNA (more than several million base pairs (bp)) remains in the well, whereas lower-molecular weight DNA fragments (several Mbp to 500 kbp) migrate into the gel and are compacted into a single band.

Cell cycle assay.

Cells were harvested and washed once with ice-cold 1xPBS. Cells were then fixed in cold 70% ethanol overnight at 4°C. Cells were washed twice with PBS and re-suspended in 1xPBS, followed by addition of RNase (100 µg/mL) and incubation at room temperature for 60 min. Propidium iodide (50µg/ml) was added to cells and incubated at room temperature for 30 min. Cell cycle was analyzed by flow cytometry as described (5).

Cell proliferation assay using BrdU incorporation

The proliferation was determined using a BrdU cell proliferation Kit (EMD Millipore, Billerica, MA) according to the manufacturer's instructions as previously described (6). Briefly, cells were seeded into 96 well-plate at 1×10^4 cells /well, followed by addition of BrdU. After 72h, cells were fixed and denatured with fixing buffer provided in the kit. The incorporated BrdU was measured using ELISA with TMB substrate and read at 450 nm.

Plating efficiency analysis.

Plating efficiency (PE) of cells was assessed as previously described (7). First, four dilutions of cells (1×10^3 , 2×10^3 , 4×10^3 , and 6×10^3) were seeded, each in triplicate, into 60-mm Petri dishes and incubated in a 37°C highly humidified atmosphere, containing 5% CO₂/95% air. After 3d incubation, the cell debris and nonattached cells were washed out using fresh warm medium. Then, cells were incubated for another 10 days. Surviving colonies were fixed and stained with 0.5% crystal violet in 20% methanol and counted. Plating efficiency (PE) was calculated as: PE= (number of colonies counted)/(number of cells plated) ×100.

Quantitative-PCR of mRNA.

For quantitative reverse transcription-PCR, total RNA was purified using TRIzol (Life Technologies, Carlsbad, CA) and the first strand cDNA was synthesized with SuperScript III (Life Technologies, Carlsbad, CA). Amplifications were carried out using SYBR green PCR mix (Bio-Rad, CA) by ABI 7500 real-time PCR system (Applied Biosystems) and the relative

quantification was performed according to the comparative Ct method. Primers used were: human Bcl2: forward, 5'-GGT GGA GGA GCT CTT CAG G-3' and reverse, 5'- ATA GTT CCA CAA AGG CAT CC-3'; human Bcl-xL: forward, 5'- ATA GTT CCA CAA AGG CAT CC -3' and reverse, 5'- TGG GAT GTC AGG TCA CTG AA-3'; human Mcl-1: forward, 5'- TAA GGA CAA AAC GGG ACT GG-3' and reverse, 5'-ACC AGC TCC TAC TCC AGC AA-3' and β -actin: forward, 5'- TCA GGA TCC ACG TGC TTG TCA -3'; reverse, 5'- TAC CCT TGG ACC CAG AGG TTC TTT GA -3'.

Mcl-1 ubiquitination measurement.

H1299 cells were transfected with HA-tagged ubiquitin construct using the NanoJuice transfection kit as described (8). After 12h, cells were subjected to double thymidine block, followed treatment with MG132 (10 μ M) for 6h and then co-IP using a Mcl-1 antibody. Mcl-1 ubiquitination was analyzed by Western blot using anti-HA antibody.

Subcellular fractionation.

Mitochondrial and nuclear fractions were isolated as previously described (8). Briefly, H1299 cells (2×10^7) were washed once with cold PBS and resuspended in isotonic mitochondrial buffer (210 mM mannitol, 70 mM sucrose, 1mM EGTA, 10mM Hepes pH 7.5) containing protease inhibitor mixture. The resuspended cells were homogenized with a polytron homogenizer (Fisher Scientific, Pittsburgh, PA) and centrifuged at 2000 \times g for 3 min to pellet the nuclei. The resulting supernatant was centrifuged at 13000 \times g for 30 min to isolate the mitochondrial pellet. Samples from each fraction were subjected to SDS-PAGE and analyzed by Western blotting.

Clonogenic survival assay.

Cells were seeded in 6-well plates or cell culture dishes. After 12 hrs, cells were treated with Hu for 24 hrs. After washing, cells were cultured in fresh regular medium for two weeks. Colonies were stained with 0.1% crystal violet in methanol and counted. Surviving colonies were counted and the surviving fraction (SF) was calculated using the formula SF = treatment colony numbers/control colony numbers after at least three independent experiments as described (5).

Generation of recombinant GST-tagged Mcl-1 proteins.

GST-tagged human Mcl-1 WT and deletion mutants were cloned into pGEX-4T-1 vector (GE healthcare) between BamH I and Sal I sites. The constructs were transformed into *Escherichia coli* Rosetta (DE3) (EMD Millipore), grown in Luria-Bertani broth at 37°C with shaking at 250 rpm and induced with 0.5 mM IPTG upon OD₆₀₀ reaching 0.4. Bacteria were then incubated at 18°C with shaking for 18 hrs, followed by lysis in buffer G (20 mM Tris-HCl pH 8.0, 150 mM NaCl and 1 mM EDTA) by sonication. After centrifugation, supernatant was applied to a glutathione sepharose column (GE healthcare) and washed with 10 column volumes of buffer G. Mcl-1 proteins were eluted with buffer (50 mM Tris-HCl, pH 8.0, 10 mM glutathione) and stored at -80°C for experimental use.

Immunoprecipitation and GST pull-down assay.

Cells were suspended in ice-cold EBC buffer (0.5% NP-40, 50 mM Tris-HCl, pH 7.6, 120 mM NaCl, 5mM CaCl₂, 5mM MgCl₂ and 1 mM β -mercaptoethanol) with protease inhibitor cocktail (EMD Biosciences, NJ), lysed by sonication followed by centrifugation at 14,000 \times g for 10 min.

The resulting supernatant was treated with 10 U micrococcal nuclease (New England Biolabs, MA) at room temperature for 20 min. After addition of EDTA (1mM), samples were incubated with agarose-conjugated Mcl-1 or Flag antibody overnight at 4°C. After washing, beads were boiled in 30 µl SDS-PAGE loading buffer for 6 min and subjected to SDS-PAGE and analyzed by Western blotting. For GST pull-down assay, GST-fused Mcl-1 proteins were incubated with glutathione sepharose 4B beads (GE healthcare) in TBS buffer (50 mM Tris-Cl, pH 7.5, 150 mM NaCl) with protease inhibitor cocktail at 4°C for 4 hrs. After washing, the beads coated with GST proteins were incubated with purified Ku proteins in TBS buffer at 4°C overnight. After washing, the samples were subjected to SDS-PAGE and analyzed by Western blotting.

Mcl-1 silencing.

Mcl-1 shRNA and siRNA were obtained from Santa Cruz Biotechnology (Santa Cruz, CA). Hairpin sequence of Mcl-1 shRNA1: 5'-GAT CCG AAG ACC ATA AAC CAA GAA TTC AAG AGA TTC TTG GTT TAT GGT CTT CTT TTT-3'; shRNA-2: 5'-GAT CCG GAC TGG CTA GTT AAA CAA TTC AAG AGA TTG TTT AAC TAG CCA GTC CTT TTT-3'; control shRNA: 5'-TTC TCC GAA CGT GTC ACG TTT CAA GAG AAC GTG ACA CGT TCG GAG AAT TTT T-3'. For pseudovirus production, Mcl-1 shRNA or control shRNA was cotransfected into 293FT cells with a lentivirus packaging plasmid mixture (pCMV-dR8.2 dvpr and pCMV-VSV-G) (System Biosciences, CA) using the NanoJuice transfection kit (EMD Chemical, Inc.) as described (9). After 48h, virus-containing medium supernatant was harvested by centrifugation at 20,000 × g. H1299 cells were infected with virus-containing media in the presence of polybrene (8 µg/ml) for 24h. Stable positive clones were selected using 1 µg/ml puromycin. Specific silencing of the targeted Mcl-1 gene was confirmed by at least three independent experiments. For silencing of Mcl-1 in H1299 cells with HR reporter, Mcl-1 siRNA (sense: 5'-GAA GAC CAU AAA CCA AGA AdTdT-3') and control siRNA (sense: 5'-UUC UCC GAA CGU GUC ACG UdTdT-3') were used for transfection with RiboJuice (EMD Millipore, Billerica, MA).

Site-directed mutagenesis and cloning.

A panel of Mcl-1 deletion mutants, including ΔN (Δ10-120), ΔPEST (Δ120-200), ΔBH1 (Δ256-265), ΔBH2 (Δ305-315), ΔBH3 (Δ213-221) and ΔTM (Δ329-346), were generated by inverse PCR using the WT Mcl-1 in pCMV-Tag2A as template. Sequences of 5'-phosphorylated primers were used for PCR as follows: ΔN, forward: 5'-TCG CCC GAA GAG GAG CTG GAC GGG-3', reverse: 5'- GAT TAC CGC GTT TCT TTT GAG GCC-3'; ΔPEST, forward: 5'-AGG TCT GGG GCC ACC AGC AGG AAG-3', reverse: 5'-CAT GAT GGC GTC AGC GGC CGG GGC-3'; ΔBH1, forward: 5'- ACT CTC ATT TCT TTT GGT GCC-3', reverse: 5'-GCT GAA AAC ATG GAT CAT CAC-3'; ΔBH2, forward: 5'- GTG GAG TTC TTC CAT GTA GAG GAC-3', reverse: 5'- GTC CCG TTT TGT CCT TAC GAG AAC-3'; ΔBH3, forward: 5'- CGC AAC CAC GAG ACG GCC TTC-3', reverse: 5'- GGT CTC CAG CGC CTT CCT GCT GG-3'; ΔTM, forward: 5'- GGT TTG GCA TAT CTA ATA AGA-3', reverse: 5'- CCT GAT GCC ACC TTC TAG GTC CTC-3'. After PCR, the amplification products were digested by Dpn I to remove the non-mutated WT Mcl-1 template, subjected to 1% agarose gel electrophoresis and purified by Qiagen gel extraction kit. Purified PCR products were circularized by ligation using T4 DNA ligase, followed by transformation into DH5α for amplification. Mcl-1 deletion mutants were confirmed by sequencing. For creation of nuclear-targeted Mcl-1 constructs, WT, ΔBH1 and BH3 mutant Mcl-1 in pCMV-Tag2A were subcloned into the pShooter-pCMV/Myc/Nuc vector

(Invitrogen, Carlsbad, CA) between the NcoI and PstI sites. Each construct was verified by sequencing.

Purification of Mre11 and Rad50 proteins from insect cells.

The Mre11-Rad50 (MR) complex was produced from Sf9 insect cells as described previously (10, 11). Briefly, Sf9 insect cells were co-infected with recombinant baculoviruses expressing Flag-hMre11 and (His)₆-hRad50, harvested and suspended in buffer F (50mM Tris-HCl pH7.4, 150mM NaCl, 1mM EDTA, 1% Triton X-100 and 10% glycerol) supplemented with protease inhibitor cocktail (EMD Biosciences, NJ) 72 hrs after infection. Cell suspensions were lysed by sonication and centrifuged at 14000×g for 10 min. Supernatants were loaded onto columns containing anti-Flag M2 antibody conjugated to agarose beads (Sigma, MO) under gravity flow. After washing with 20 column volumes of buffer F, bound MR complex was eluted with 200 µg/ml 3 × flag peptide (Sigma, MO) in buffer F. Eluted MR proteins were stored at -80°C.

ChIP assay following I-SceI-induced DSBs.

To compare binding efficiency of Ku 70 or Mre11 on DSB ends generated by I-SceI homing-endonuclease, pCBASceI plasmids were transfected into MEF cells containing pDR-GFP as described (12). After 24 hrs, chromatin immunoprecipitation (ChIP) assay was performed using Pierce Agarose ChIP Kit (Thermo Scientific, USA) and Mre 11 and Ku70 antibodies according to the manufacturer's protocol. Mre11- or Ku70-associated DNA was analyzed by PCR using primer 1 or primer 2 upstream or downstream of I-SceI site, respectively. Primer 1: forward, 5'-TAC AGC TCC TGG GCA ACG TG-3'; reverse, 5'-TCC TGC TCC TGG GCT TCT CG-3'. Primer 2: forward, 5'-CGT CCA GGA GCG CAC CAT CTT CTT-3'; reverse, 5'-ATC GCG CTT CTC GTT GGG GTC TTT-3'. The PCR products were analyzed on a 1.2% agarose gel. Mre11- or Ku70-associated DNA was also quantified by real-time PCR using SYBR Green supermix (Bio-Rad, Hercules, CA) on an ABI 7500 system (Applied Biosystems, Foster City, CA) and the comparative C_T (Δ ΔC_T) program. Input controls were used to normalize the DNA samples. Primer sequences: forward, 5'-GTG ACC ACC CTG ACC TAC GG-3'; reverse: 5'-AAG TCG TGC TGC TTC ATG TG-3'.

Electrophoretic mobility shift assay (EMSA).

Double-strand DNA (dsDNA) end binding of proteins was assessed by EMSA as described previously (13, 14). Oligonucleotides were chemically synthesized and purified by HPLC (IDT, Coralville, Iowa). The sequences of oligonucleotides were: TP423: 5' -CTG CAG GGT TTT TGT TCC AGT CTG TAG CAC TGT GTA AGA CAG GCC AGA TC-3'; and TP424: 5'-CAC AGT GCT ACA GAC TGG AAC AAA AAC CCT GCA GTA CTC TAC TCA TCT C- 3'. First, the 5' end of TP423 was labeled with [γ -³²P]-ATP and polynucleotide kinase (New England Biolabs, Ipswich, MA). Non-labeled [γ -³²P]-ATP was removed using G-25 Spin Columns. The 3' overhanging DNA duplexes were produced by annealing of TP423 and TP424 oligonucleotides. The resulted 3' overhanging DNA duplexes (10 nM) were incubated with Ku70/80 or MR in absence or presence of increasing concentrations of Mcl-1 in buffer (25 mM MOPS (pH7.0), 50 mM KCl, 1 mM DTT, and 1 mM MnCl₂) at room temperature for 15 min. DNA loading buffer (R0611, Thermo Scientific) was added to samples, subjected to 6% non-denaturing TBE (Tris-borate-EDTA)-polyacrylamide gel and analyzed by Typhoon 9210 phosphorimager (GE Healthcare).

Thermal shift assay.

Thermal shift assay was employed for screening of potential Mcl-1 binding compound candidates. Experiments were carried out using protein thermal shift dye kit (Thermo Fisher Scientific) according to the manufacturer's instructions (15). Briefly, 2 µg of GST-Mcl-1 WT protein was incubated with different compounds in the reaction buffer and fluorescence was collected by melt curve program of the 7500 fast real-time PCR systems. Data were analyzed using protein thermal shift software v1.0 (Thermo Fisher Scientific).

Isothermal titration calorimetry (ITC).

The binding affinity of MI-223 with Mcl-1 protein was examined by isothermal titration calorimetry (ITC) assay as described (16). ITC assay was carried out in the auto-iTC200 instrument (MicroCal, GE) at 25 °C. Mcl-1 WT or BH1 deletion mutant protein was loaded into a 96 Deepwell PP plate. MI-223 compound was then titrated stepwise into the protein for a total of 16 injections. Reference power and initial delay were set as 5 µCal/sec and 60s, respectively. A string speed of 750 rpm was used for the ITC measurements. The binding constant (K_d) value was determined by fitting the titration curve to a one-site binding mode, using the Origin software provided by the manufacturer.

Fluorescence polarization assay.

Puma BH3 peptide has been reported to specifically bind the BH1 domain of Mcl-1 (17), thus we chose fluorescence polarization (FP) to monitor the interaction of MI-223 with Mcl-1 BH1 domain, leading to depolarization of fluorescent-labeled Puma peptide. 5 nM of fluorescent Puma BH3 peptide (TAMRA-EEWAREIGAQLRRMADDLNAQYER) was incubated with Mcl-1 protein (20 nM) in the absence or presence of increasing concentrations of MI-223 in the binding buffer [50 mM Tris (pH 8.0), 150 mmol/L NaCl, 0.1% bovine serum albumin (BSA), and 5 mM DTT] in black 1,536-well microplates. Plates were incubated at room temperature for 1h and FP values (in millipolarization units) were measured using Envision multi-label plate reader (PerkinElmer). The excitation filter was at 540 ± 20 nm and emission filter at 590 ± 20 nm. Data analysis and inhibitory constant (K_i) value was determined by GraphPad prism software as described (18).

Immunohistochemistry.

Tumor tissues were fixed in formalin, embedded in paraffin and cut into 5 µm-thick sections. After deparaffinization, rehydration, inactivation of endogenous peroxidase and antigen retrieval, the IHC staining were performed using R.T.U Vectastain Kit (Vector Laboratories) according to manufacturer's instructions using Ki67(1:500, abcam), γ -H2AX(1:300, EMD Millipore) antibodies. Ki67- or γ -H2AX- positive cells in tumor tissues were scored at 400 × magnification. The average number of positive cells per 0.0625 mm² area was determined from three separate fields in each of three independent tumor samples.

Mouse blood analysis.

Whole blood (250µL) was collected in EDTA-coated tubes via cardiac puncture of anesthetized mice for hematology studies. Specimens were analyzed for white blood cells (WBC), red blood cells (RBC), platelets (PLT), alanine aminotransferase (ALT), aspartate aminotransferase (AST) and blood urea nitrogen (BUN) in the Clinical Pathology Laboratory at the University of Georgia (Athens, GA) as described (19).

Supplemental References

1. Ikonen E, Fiedler K, Parton RG, and Simons K. Prohibitin, an antiproliferative protein, is localized to mitochondria. *FEBS Lett.* 1995;358(3):273-7.
2. Mihara M, Erster S, Zaika A, Petrenko O, Chittenden T, Pancoska P, and Moll UM. p53 has a direct apoptogenic role at the mitochondria. *Mol Cell.* 2003;11(3):577-90.
3. Hanada K, Budzowska M, Davies SL, van Drunen E, Onizawa H, Beverloo HB, Maas A, Essers J, Hickson ID, and Kanaar R. The structure-specific endonuclease Mus81 contributes to replication restart by generating double-strand DNA breaks. *Nat Struct Mol Biol.* 2007;14(11):1096-104.
4. Ray Chaudhuri A, Hashimoto Y, Herrador R, Neelsen KJ, Fachinetti D, Bermejo R, Cocito A, Costanzo V, and Lopes M. Topoisomerase I poisoning results in PARP-mediated replication fork reversal. *Nature structural & molecular biology.* 2012;19(4):417-23.
5. You S, Li R, Park D, Xie M, Sica GL, Cao Y, Xiao ZQ, and Deng X. Disruption of STAT3 by niclosamide reverses radioresistance of human lung cancer. *Mol Cancer Ther.* 2014;13(3):606-16.
6. Kumar S, Sharghi-Namini S, Rao N, and Ge R. ADAMTS5 functions as an anti-angiogenic and anti-tumorigenic protein independent of its proteoglycanase activity. *The American journal of pathology.* 2012;181(3):1056-68.
7. Goodheart CR, Castro BC, Giviers A, and Regnier PR. Plating efficiency for primary hamster embryo cells as an index of efficacy of fetal bovine serum for cell culture. *Appl Microbiol.* 1973;26(4):525-8.
8. Wang B, Xie M, Li R, Owonikoko TK, Ramalingam SS, Khuri FR, Curran WJ, Wang Y, and Deng X. Role of Ku70 in deubiquitination of Mcl-1 and suppression of apoptosis. *Cell death and differentiation.* 2014;21(7):1160-9.
9. Huang S, Okumura K, and Sinicrope FA. BH3 mimetic obatoclax enhances TRAIL-mediated apoptosis in human pancreatic cancer cells. *Clin Cancer Res.* 2009;15(1):150-9.
10. Lee JH, and Paull TT. Purification and biochemical characterization of ataxia-telangiectasia mutated and Mre11/Rad50/Nbs1. *Methods in enzymology.* 2006;408(529-39).
11. Xie M, Park D, You S, Li R, Owonikoko TK, Wang Y, Doetsch PW, and Deng X. Bcl2 inhibits recruitment of Mre11 complex to DNA double-strand breaks in response to high-linear energy transfer radiation. *Nucleic Acids Res.* 2015;43(2):960-72.
12. Pei H, Zhang L, Luo K, Qin Y, Chesi M, Fei F, Bergsagel PL, Wang L, You Z, and Lou Z. MMSET regulates histone H4K20 methylation and 53BP1 accumulation at DNA damage sites. *Nature.* 2011;470(7332):124-8.
13. Yu Z, Vogel G, Coulombe Y, Dubeau D, Spehalski E, Hebert J, Ferguson DO, Masson JY, and Richard S. The MRE11 GAR motif regulates DNA double-strand break processing and ATR activation. *Cell research.* 2012;22(2):305-20.
14. Lee JH, Ghirlando R, Bhaskara V, Hoffmeyer MR, Gu J, and Paull TT. Regulation of Mre11/Rad50 by Nbs1: effects on nucleotide-dependent DNA binding and association with ataxia-telangiectasia-like disorder mutant complexes. *The Journal of biological chemistry.* 2003;278(46):45171-81.

15. Jin L, Li D, Alesi GN, Fan J, Kang HB, Lu Z, Boggon TJ, Jin P, Yi H, Wright ER, et al. Glutamate dehydrogenase 1 signals through antioxidant glutathione peroxidase 1 to regulate redox homeostasis and tumor growth. *Cancer Cell*. 2015;27(2):257-70.
16. Gu L, Zhang H, Liu T, Zhou S, Du Y, Xiong J, Yi S, Qu CK, Fu H, and Zhou M. Discovery of Dual Inhibitors of MDM2 and XIAP for Cancer Treatment. *Cancer Cell*. 2016;30(4):623-36.
17. Mei Y, Du W, Yang Y, and Wu M. Puma(*)Mcl-1 interaction is not sufficient to prevent rapid degradation of Mcl-1. *Oncogene*. 2005;24(48):7224-37.
18. Park D, Magis AT, Li R, Owonikoko TK, Sica GL, Sun SY, Ramalingam SS, Khuri FR, Curran WJ, and Deng X. Novel small-molecule inhibitors of Bcl-XL to treat lung cancer. *Cancer Res*. 2013;73(17):5485-96.
19. Han B, Park D, Li R, Xie M, Owonikoko TK, Zhang G, Sica GL, Ding C, Zhou J, Magis AT, et al. Small-Molecule Bcl2 BH4 Antagonist for Lung Cancer Therapy. *Cancer Cell*. 2015;27(6):852-63.

Uncropped/unedited gel and blot images

Full unedited gel for Figure 1

Figure 1B

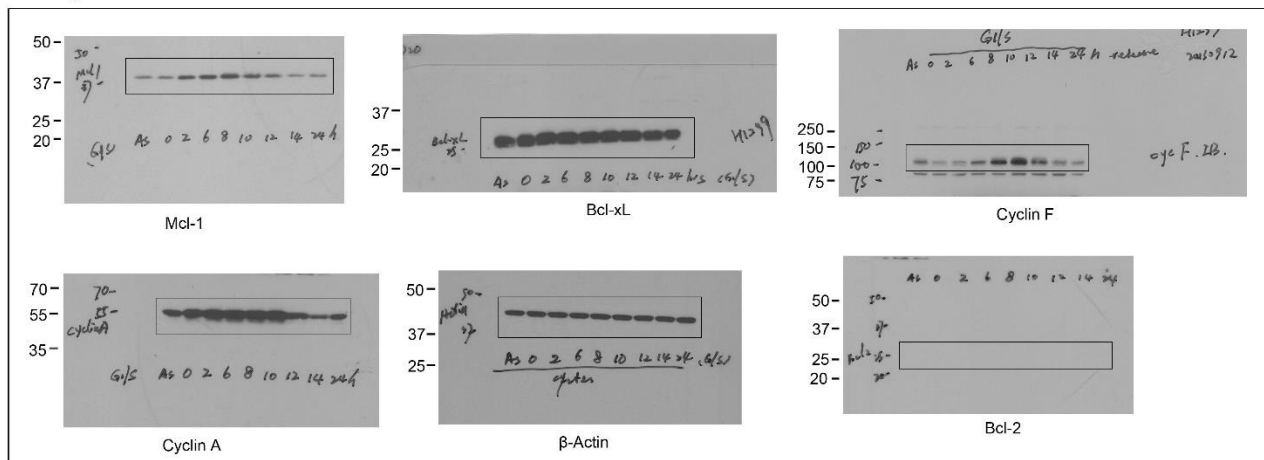
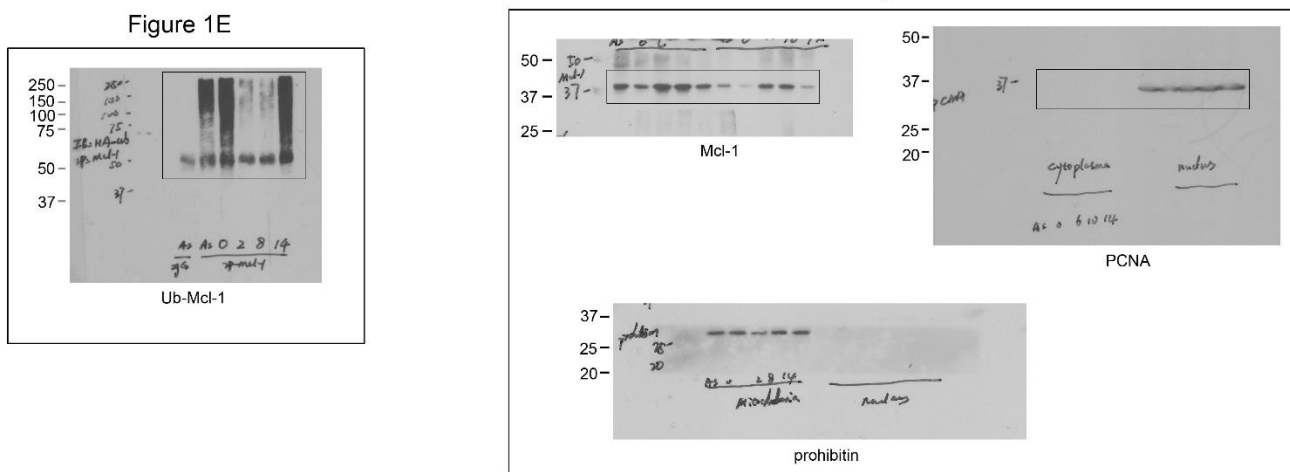
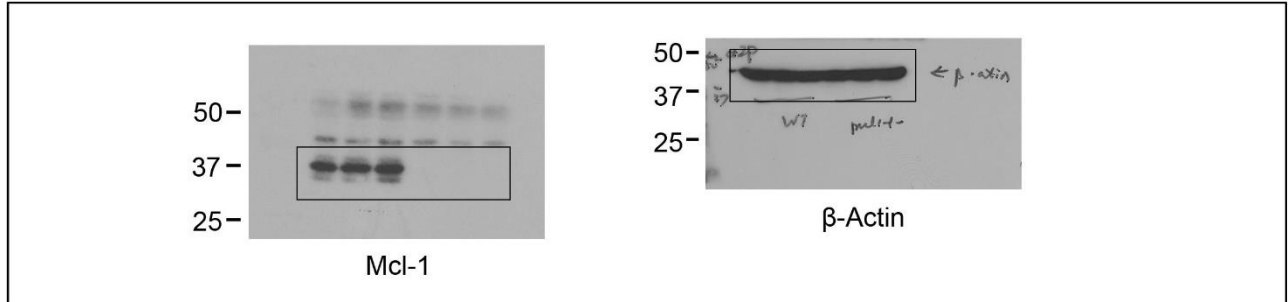


Figure 1F



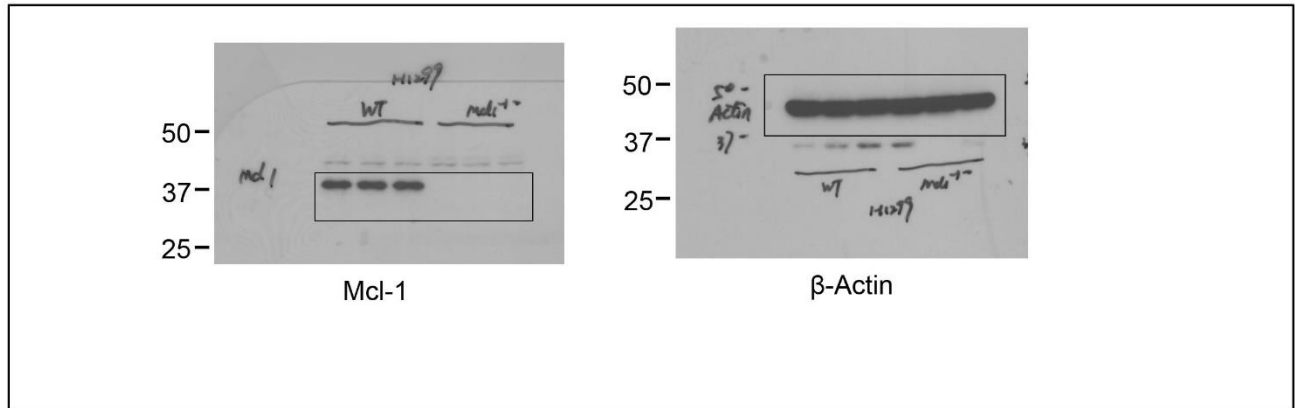
Full unedit gel for Figure 2

Figure 2A



Full unedit gel for Figure 3

Figure 3A



Full unedit gel for Figure 4

Figure 4B

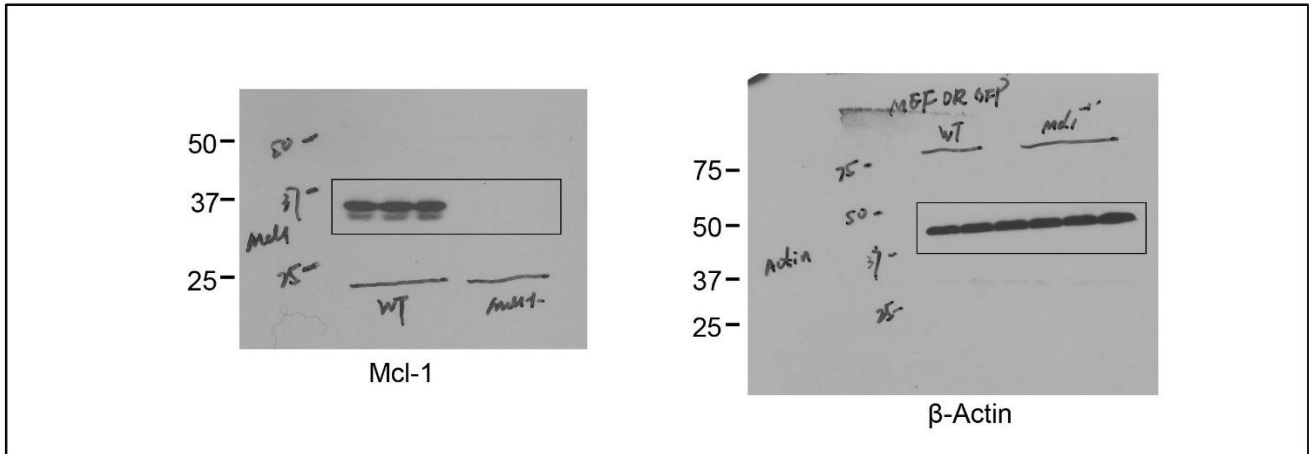
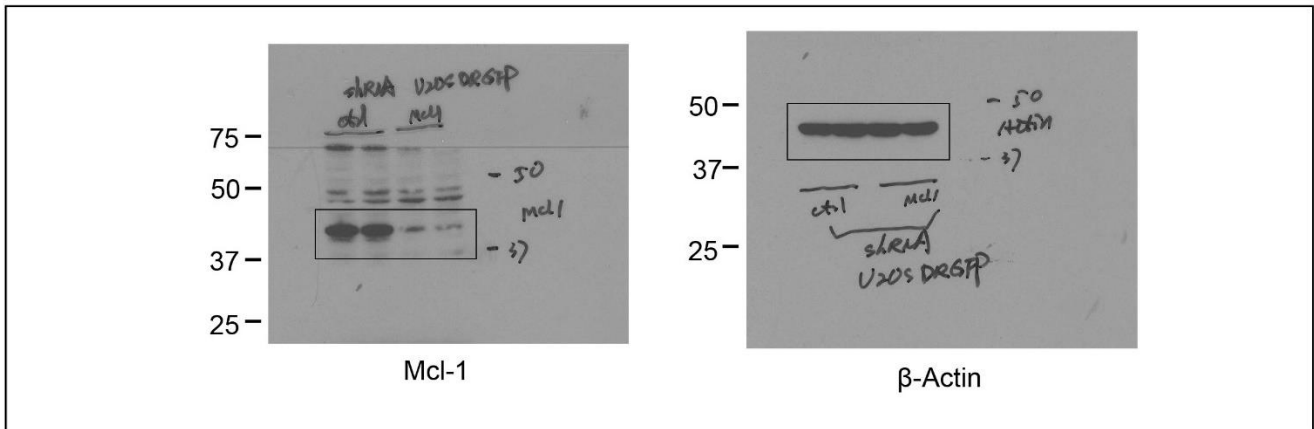


Figure 4C



Full unedit gel for Figure 5
Figure 5B

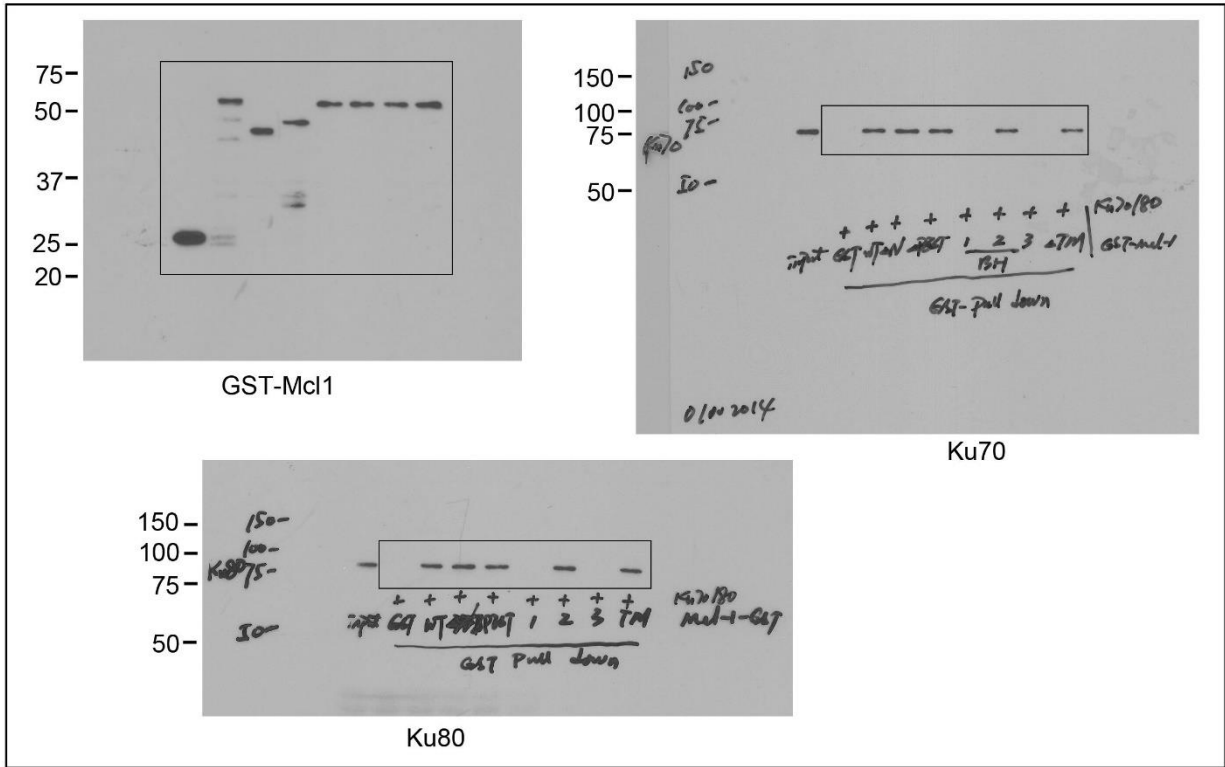
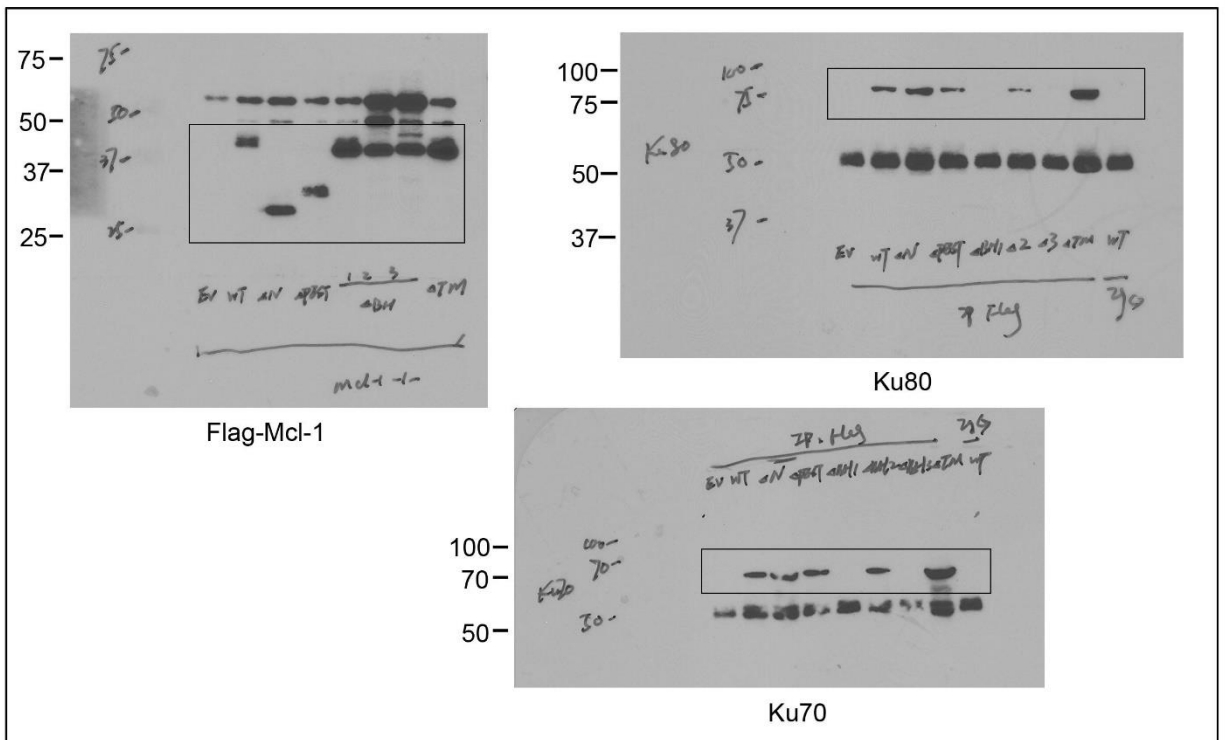
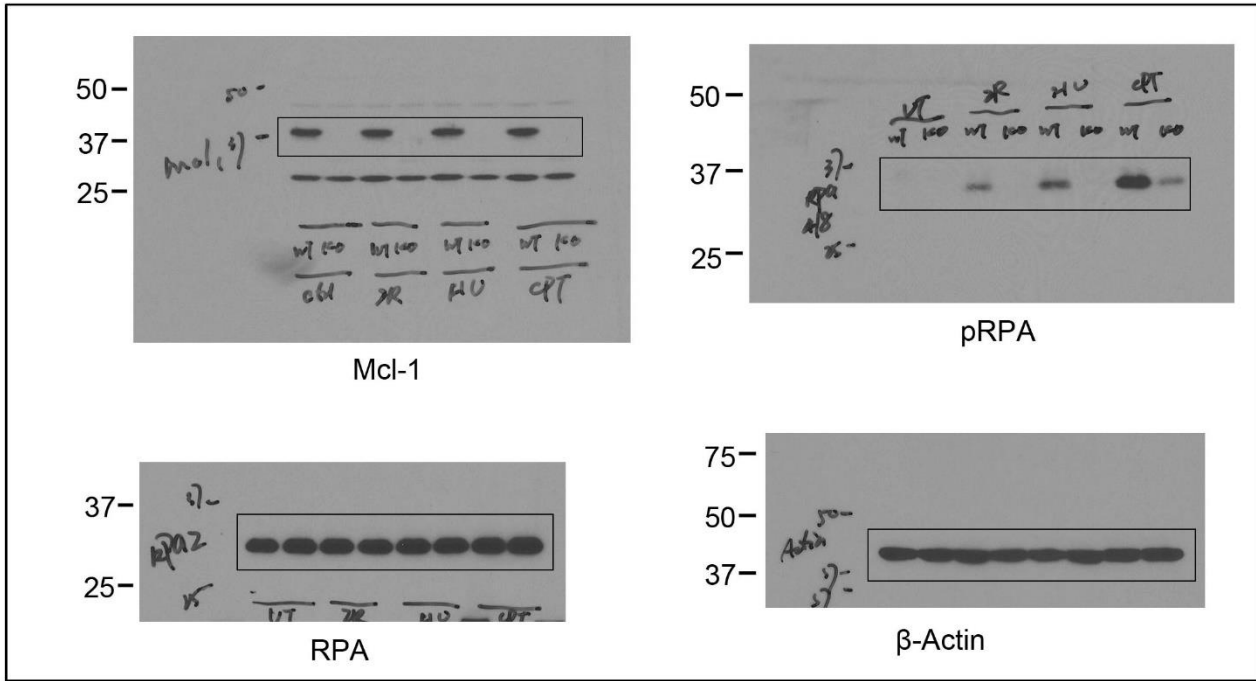


Figure 5C



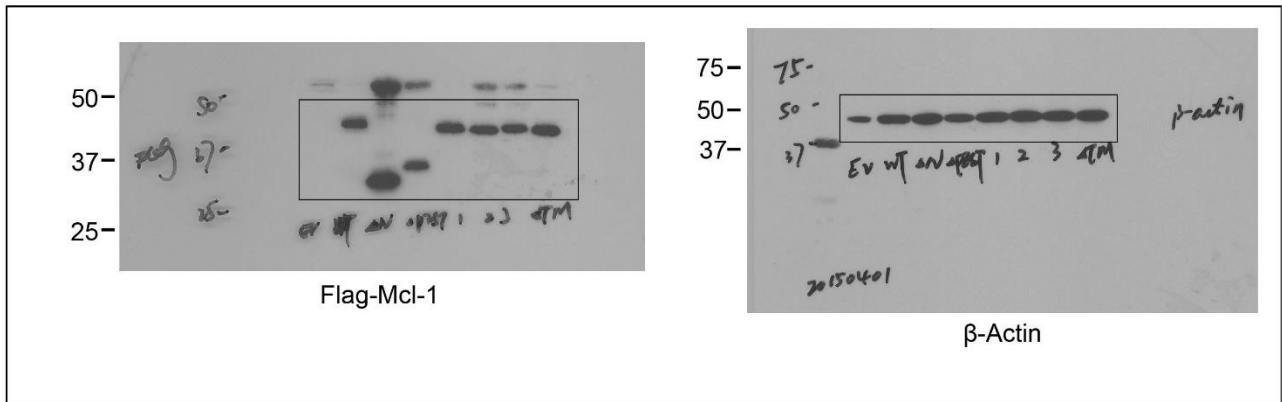
Full unedit gel for Figure 6

Figure 6D



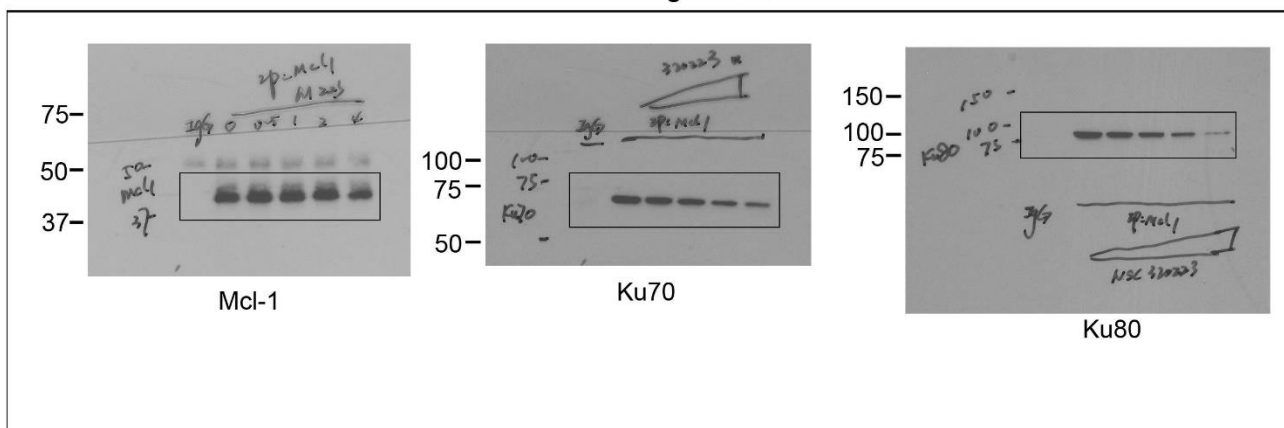
Full unedit gel for Figure 7

Figure 7A



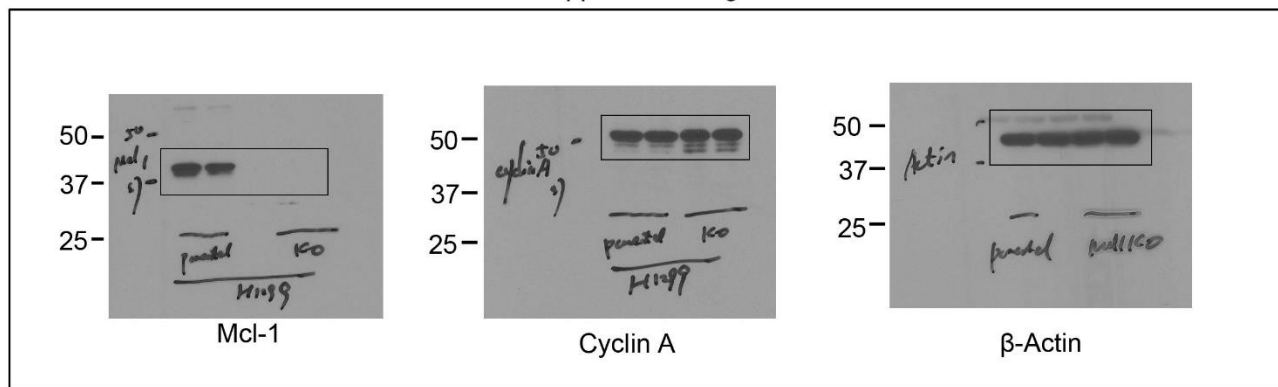
Full unedit gel for Figure 8

Figure 8E

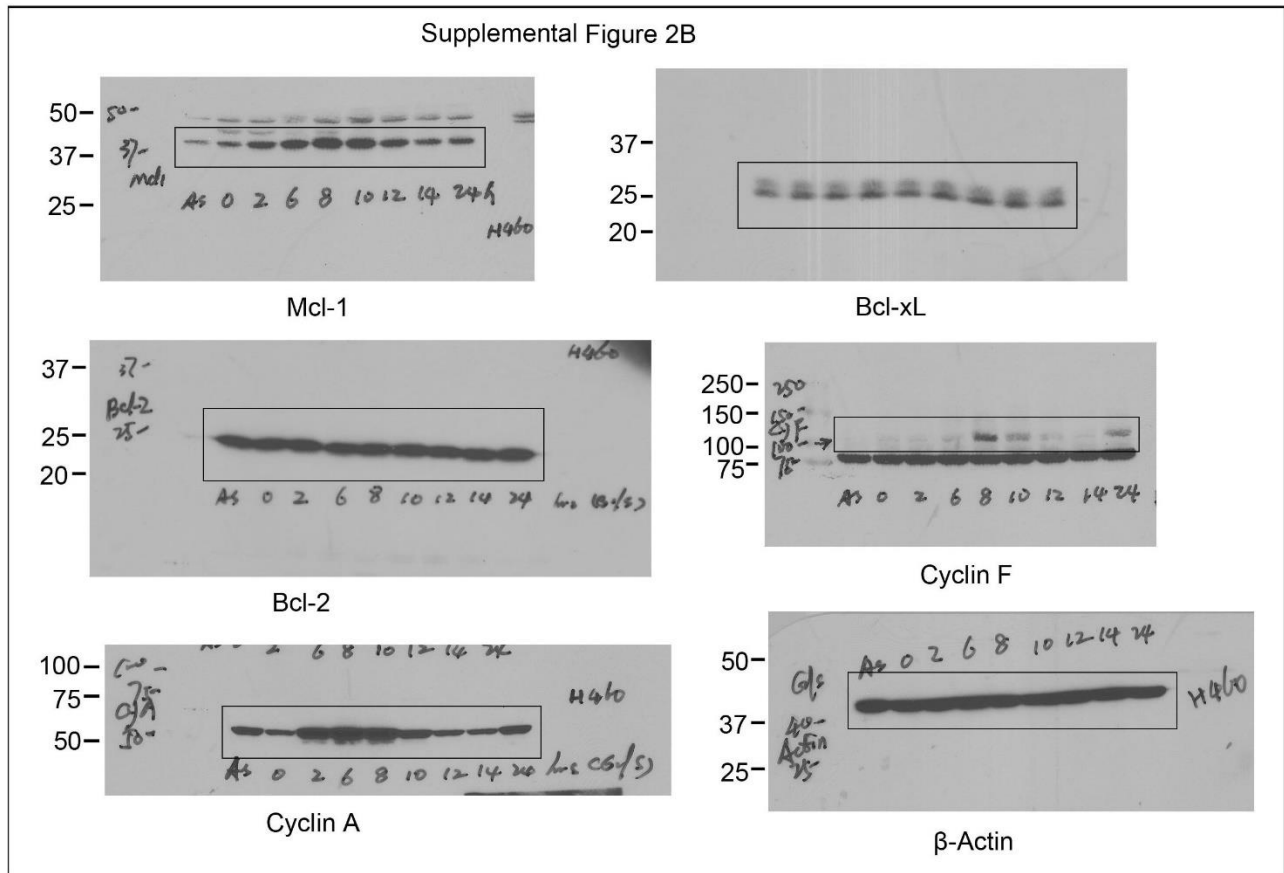


Full unedit gel for Supplemental Figure 1

Supplemental Figure 1A

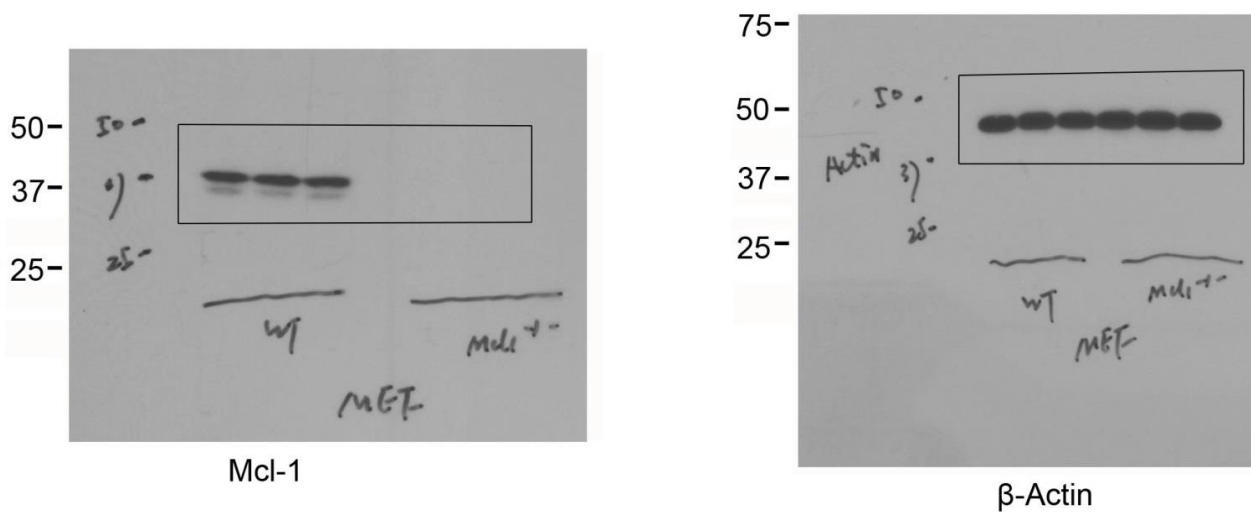


Full unedited gels for Supplemental Figure 2



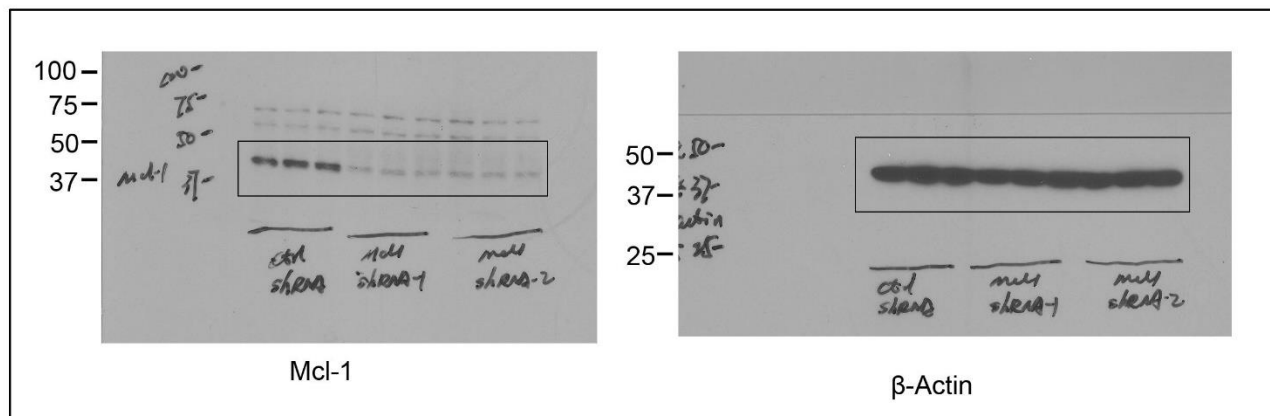
Full unedit gel for Supplemental Figure 3

Supplemental Figure 3A



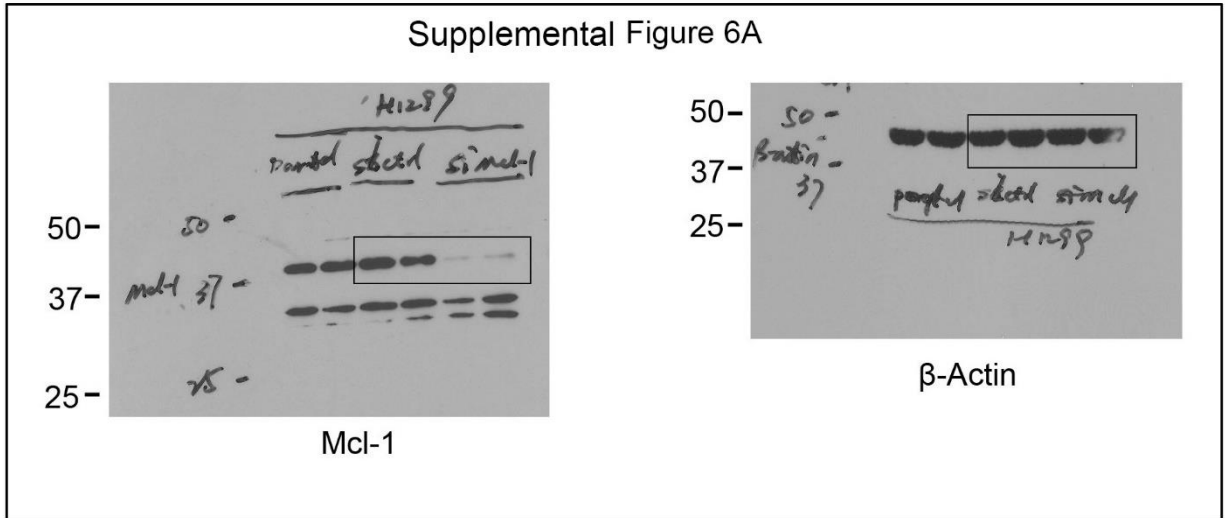
Full unedit gel for supplemental Figure 4

Supplemental Figure 4B

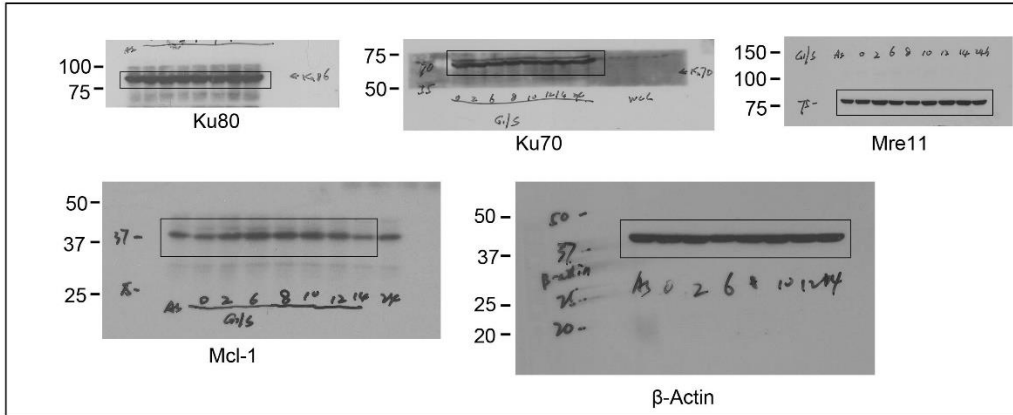


Full unedit gel for Supplemental Figure 6

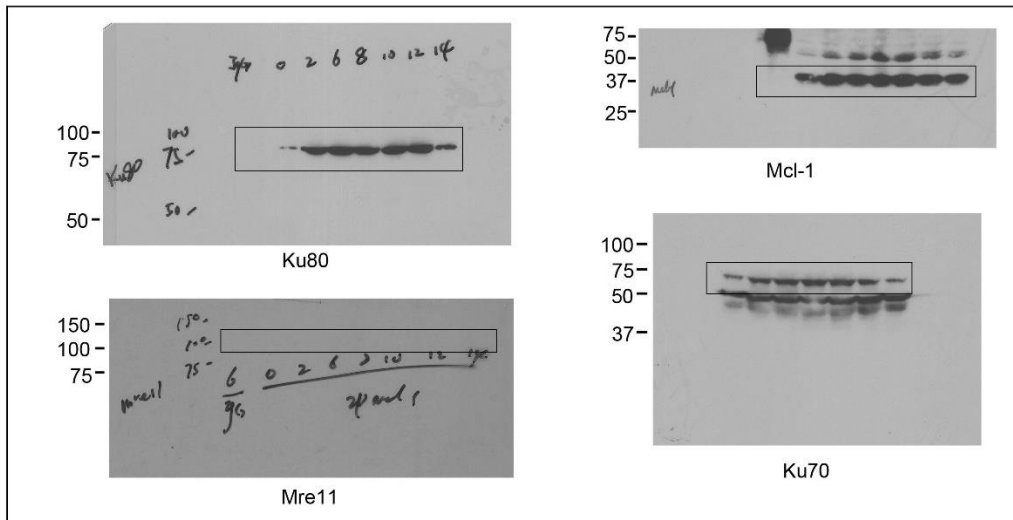
Supplemental Figure 6A



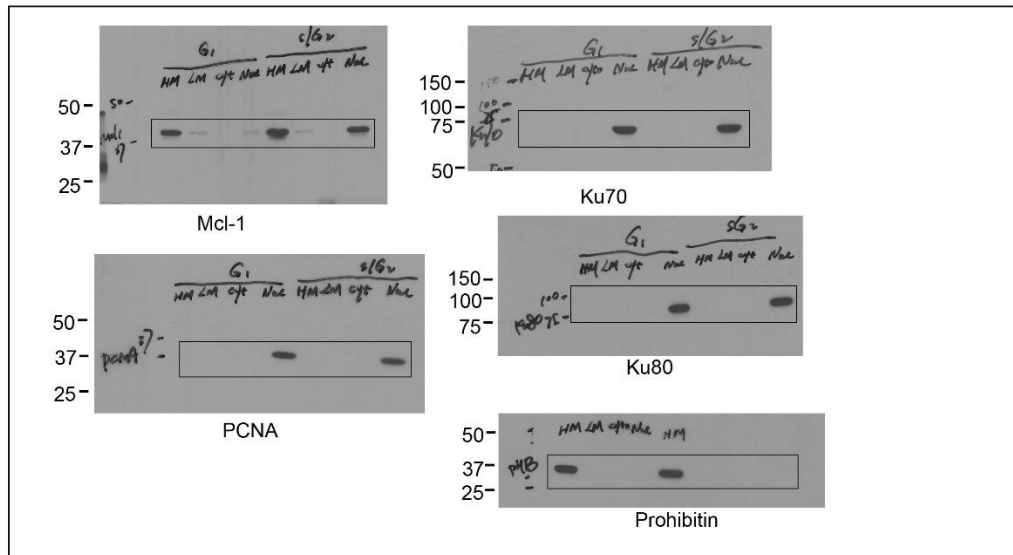
Full unedited gel for Supplemental Figure 7
 Supplemental Figure 7D



Supplemental Figure 7E

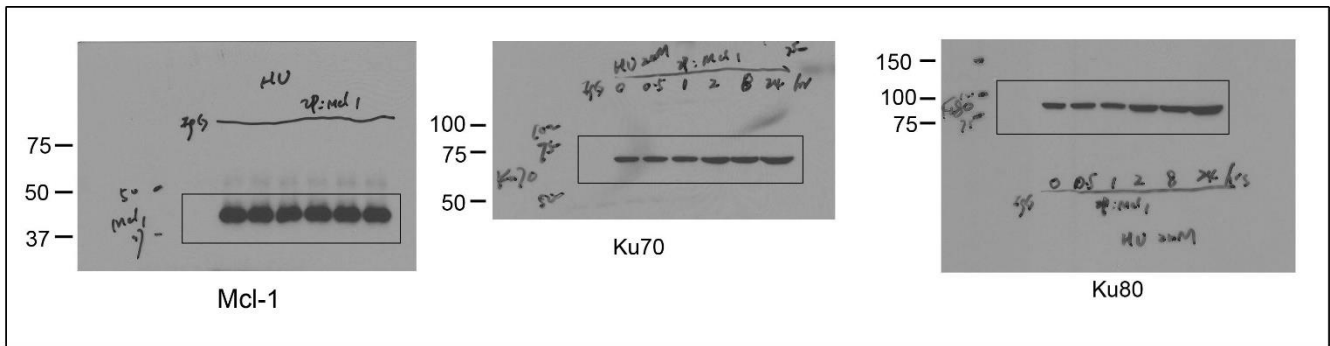


Supplemental Figure 7F

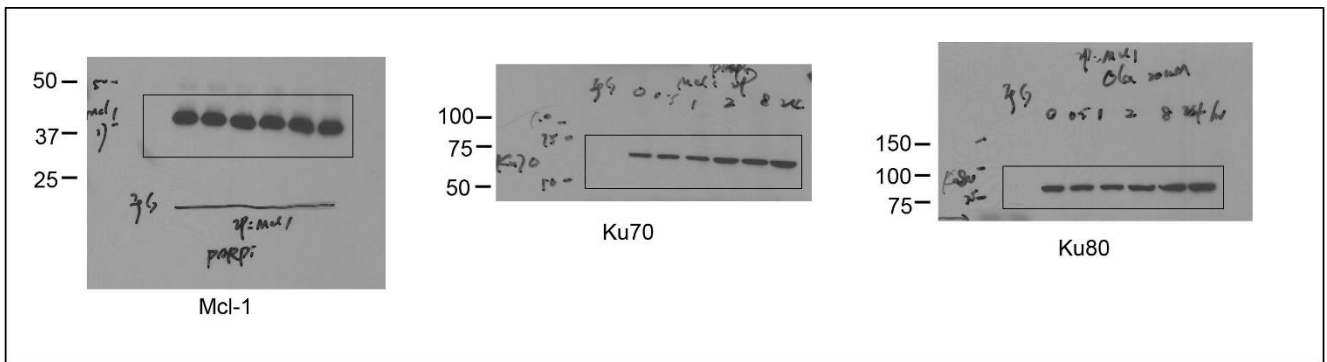


Full unedit gel for supplemental Figure 8

Supplemental Figure 8A

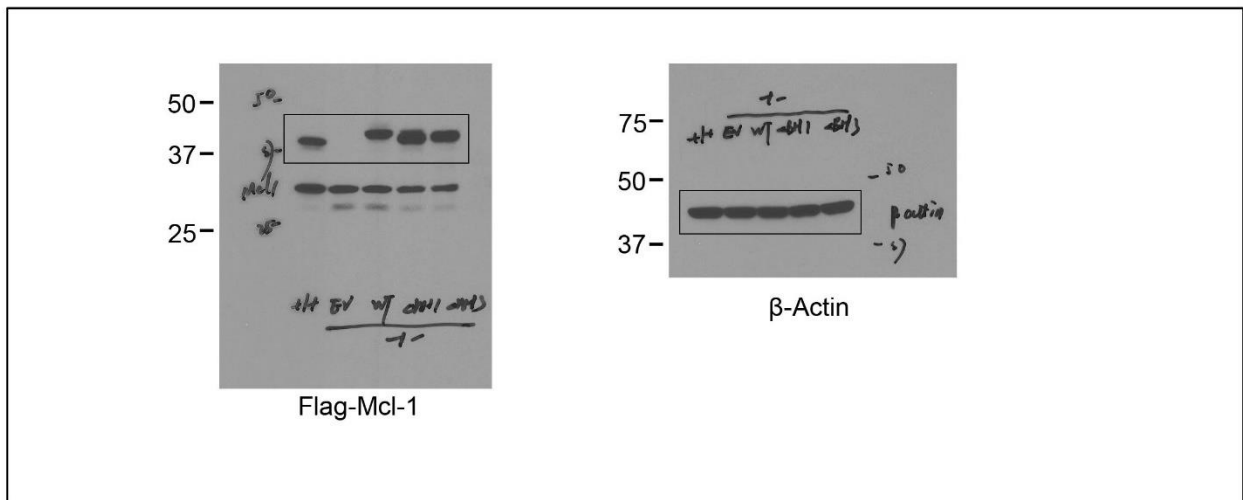


Supplemental Figure 8B



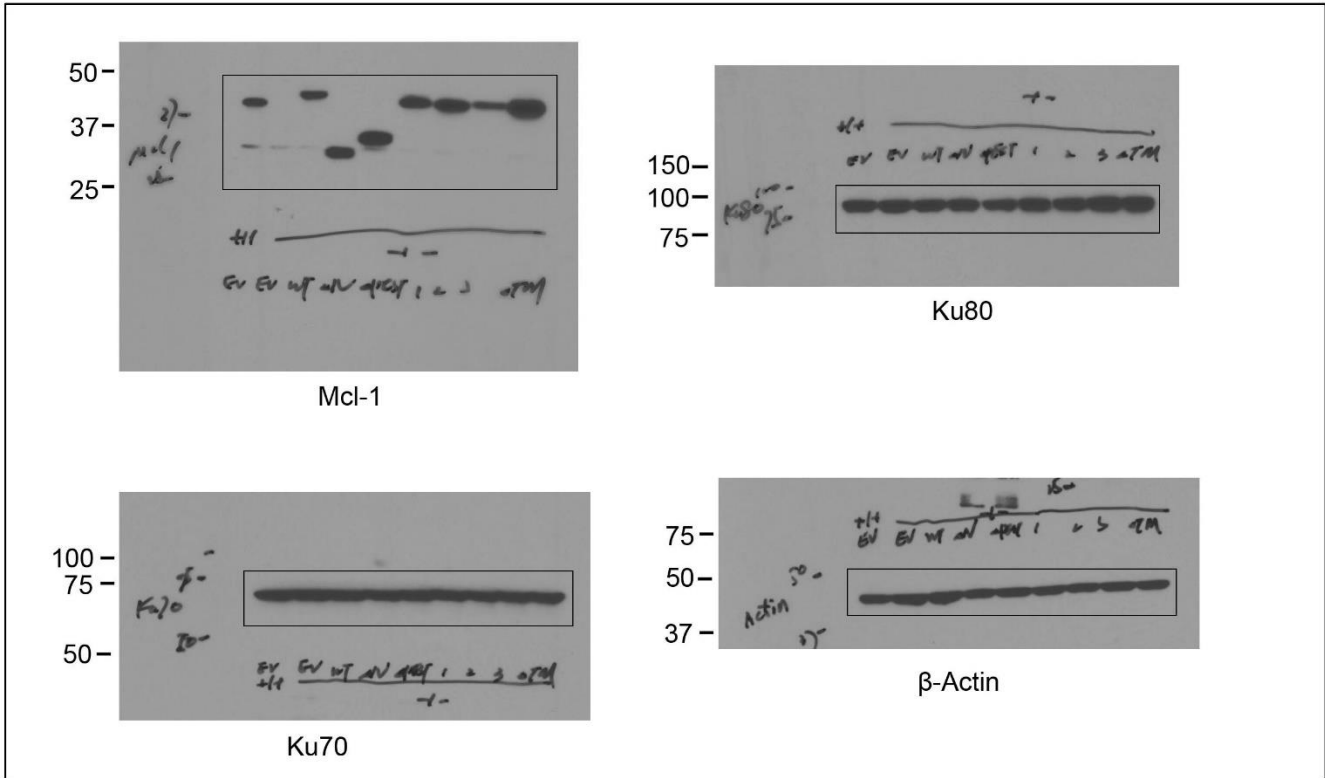
Full unedit gel for supplemental Figure 11

Supplemental Figure 11A



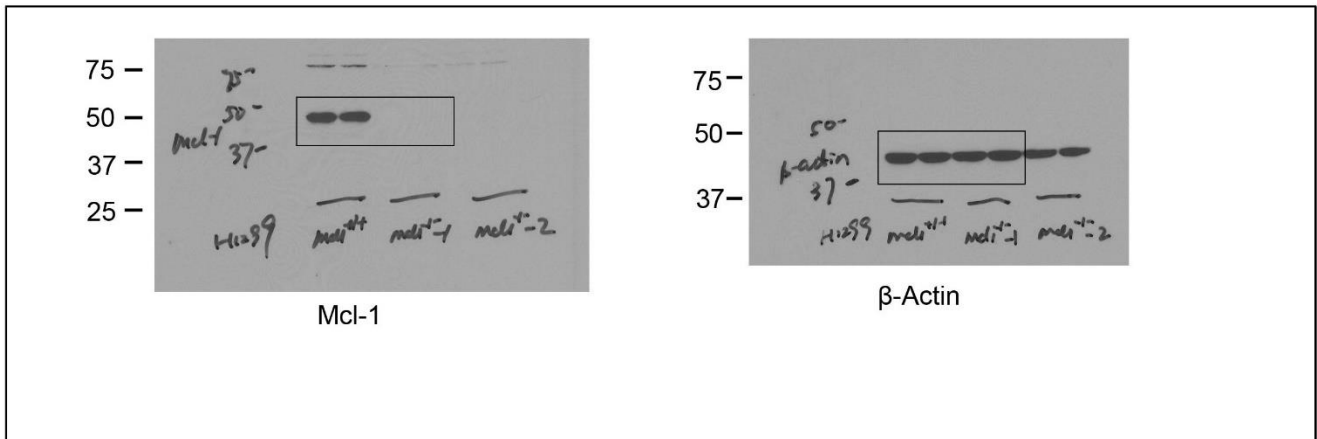
Full unedit gel for supplemental Figure13

Supplemental Figure 13A

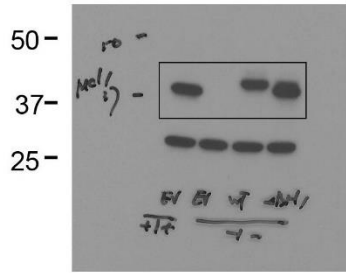


Full unedit gel for supplemental Figure 15

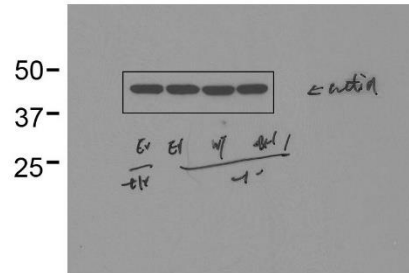
Supplemental Figure 15A



Full unedit gel for supplemental Figure 16
Supplemental Figure 16B



Mcl-1



β -Actin